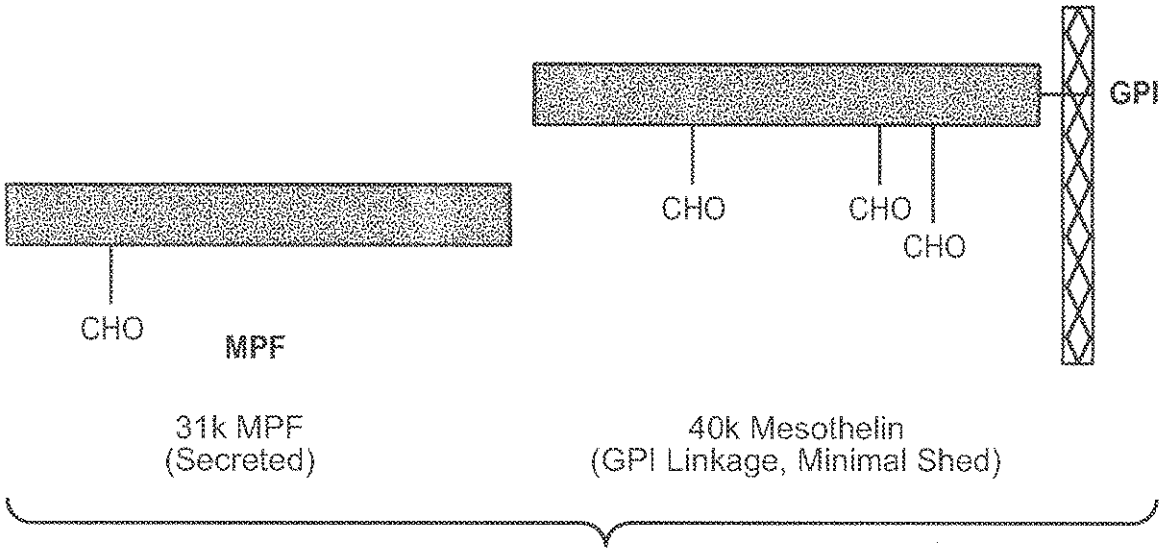

GPI
CHO
CHO
CHO
CHO
MPF
31k MPF
(Secreted)
40k Mesothelin
(GPI Linkage, Minimal Shed)

FIG. 1

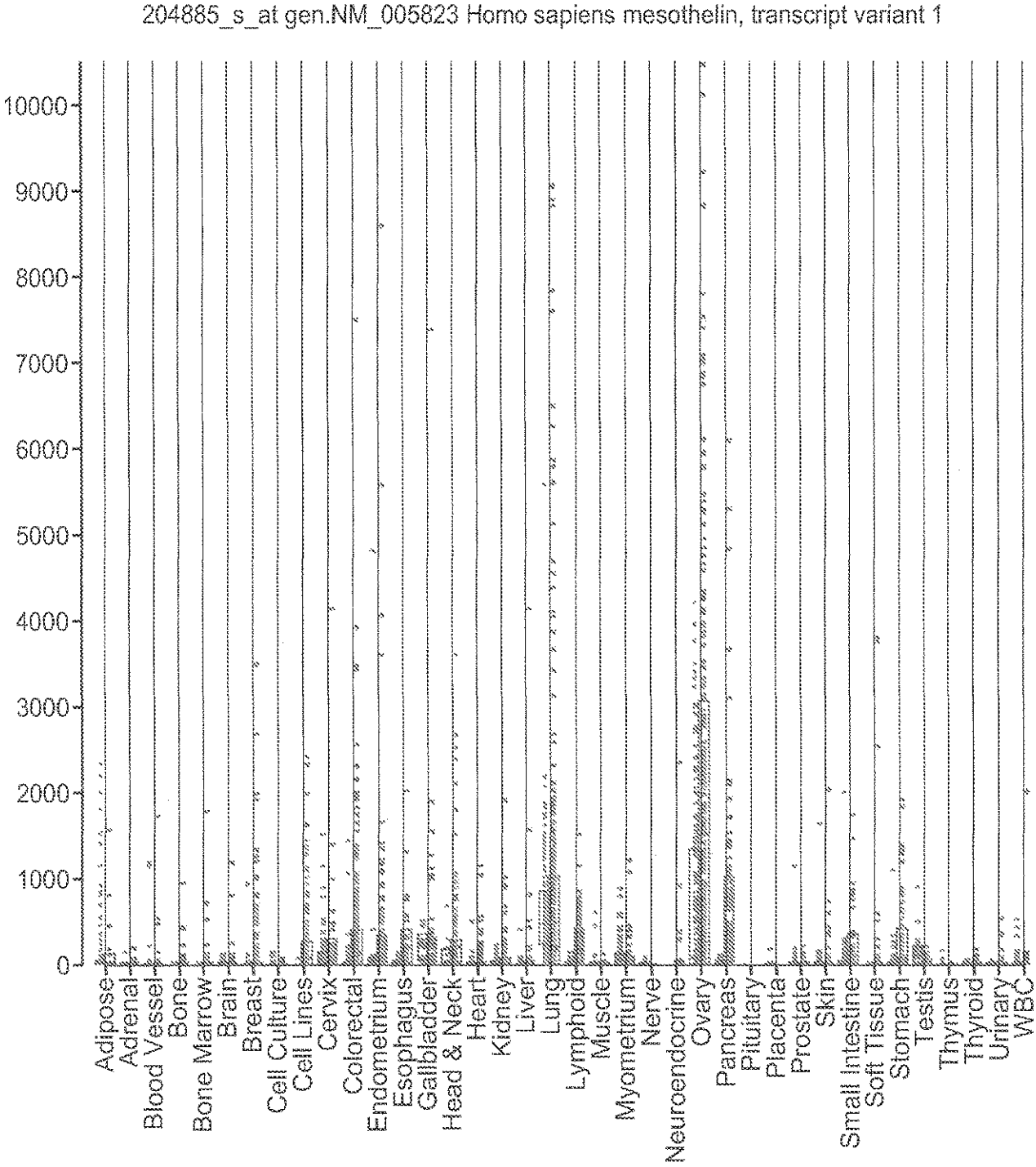

204885_s_at gen.NM_005823 Homo sapiens mesothelin, transcript variant 1
10000
9000
8000
7000
6000
5000
4000
3000
2000
1000
0
Adipose
Adrenal
Blood Vessel
Bone
Bone Marrow
Brain
Breast
Cell Culture
Cell Lines
Cervix
Colorectal
Endometrium
Esophagus
Gallbladder
Head & Neck
Heart
Kidney
Liver
Lung
Lymphoid
Muscle
Myometrium
Nerve
Neuroendocrine
Ovary
Pancreas
Pituitary
Placenta
Prostate
Skin
Small Intestine
Soft Tissue
Stomach
Testis
Thymus
Thyroid
Urinary
WBC

FIG. 2

Anti-mesothelin Monoclonal Antibodies

mAb	Isotype	Epitope Group	Epitope Region	Blocks muc16 Binding?	Kd (nM) Biacore
7D9	G1	A	152-175	Enhances	0.23
19C3	G2b	C	1-70	YES	0.06
2E5	G2	C	1-70	YES	0.49
8B11	G1	B1	71-131	No	138
17A5	G1	B1	71-131	No	n.d.
11H8	G2b	B1	71-131	No	n.d.
16D5	G2a	B2	71-131	Enhances	2.21
18D12	G2b	B3	131-178	No	n.d.
3H2	G1	B	71-131	Enhances	n.d.
22A10	G2a	D	209-212	Enhances	4.25
15F7	G2a	E	1-131	No	n.d.
12F6	G2a	E	n.d.	n.d.	780

FIG. 3

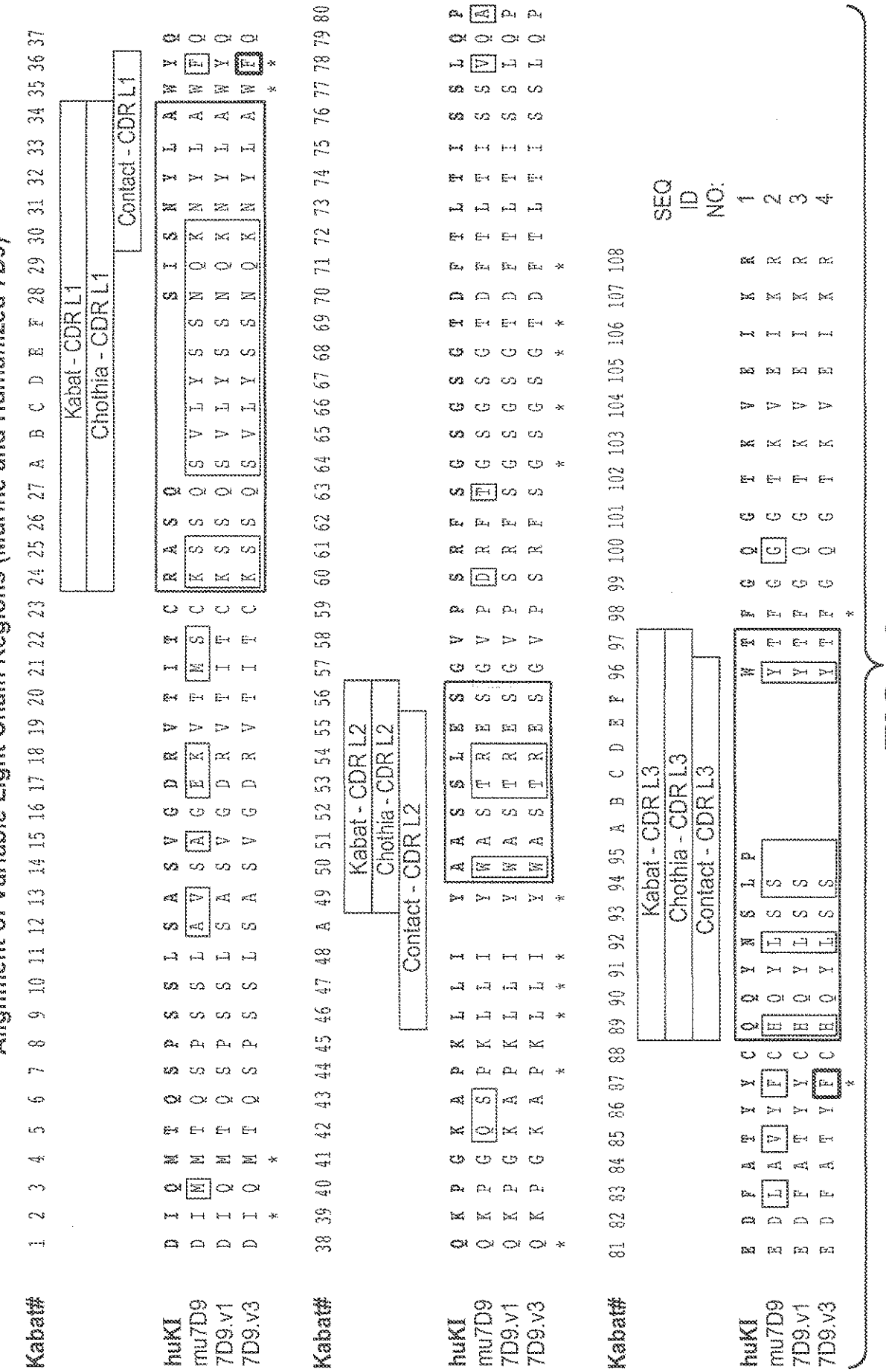

Alignment of Variable Light Chain Regions (Murine and Humanized 7D9)
Kabat - CDR L1
Chothia - CDR L1
Contact - CDR L1
Kabat - CDR L2
Chothia - CDR L2
Contact - CDR L2
Kabat - CDR L3
Chothia - CDR L3
Contact - CDR L3
SEQ ID NO:
huKI
mu7D9
7D9.v1
7D9.v3
Kabat#

FIG. 4

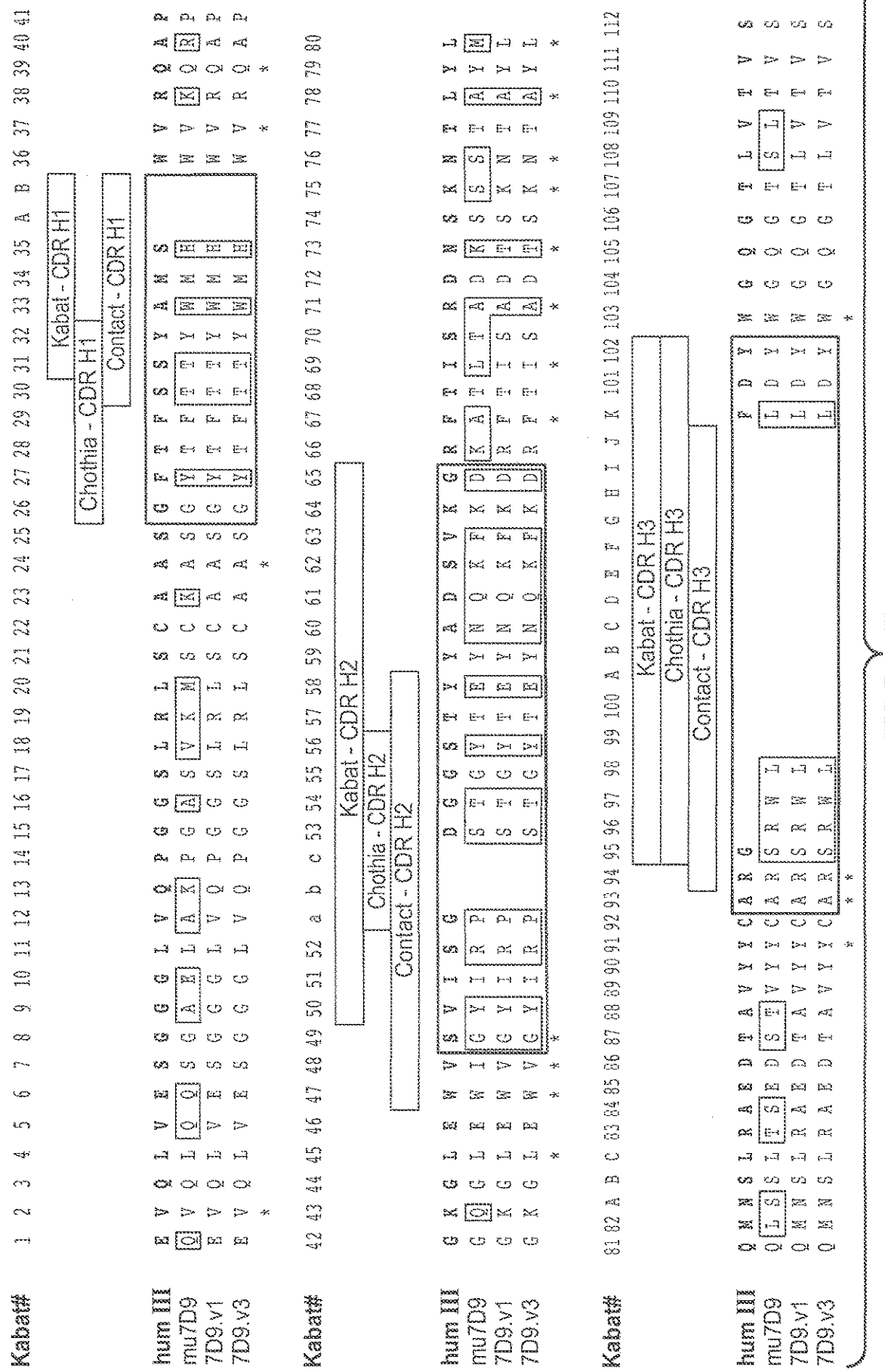

Alignment of Variable Heavy Chain Regions (Murine and Humanized 7D9)
Kabat - CDR H1
Chothia - CDR H1
Contact - CDR H1
Kabat - CDR H2
Chothia - CDR H2
Contact - CDR H2
Kabat - CDR H3
Chothia - CDR H3
Contact - CDR H3
SEQ ID NO:

FIG. 5

Chimeric and Humanized Variants of 7D9

	LC	HC	KD (nM) Over Human MSLN
Chimeric 7D9	Chimeric	Chimeric	1.84
7D9.v1	V_{kI} Graft	VH_{ATA} Graft	3.98
7D9.v2	Y36F, Y87F	V48I, F67A, I69L, K75S, N76S and L80M	1.78
7D9.v3	Y36F, Y87F	VH_{ATA} Graft	1.9
7D9.v4	V_{kI} Graft	V48I, F67A, I69L, K75S, N76S and L80M	3.01
7D9.v5	Y36F	VH_{ATA} Graft	3.49
7D9.v6	Y87F	VH_{ATA} Graft	4.08

FIG. 6

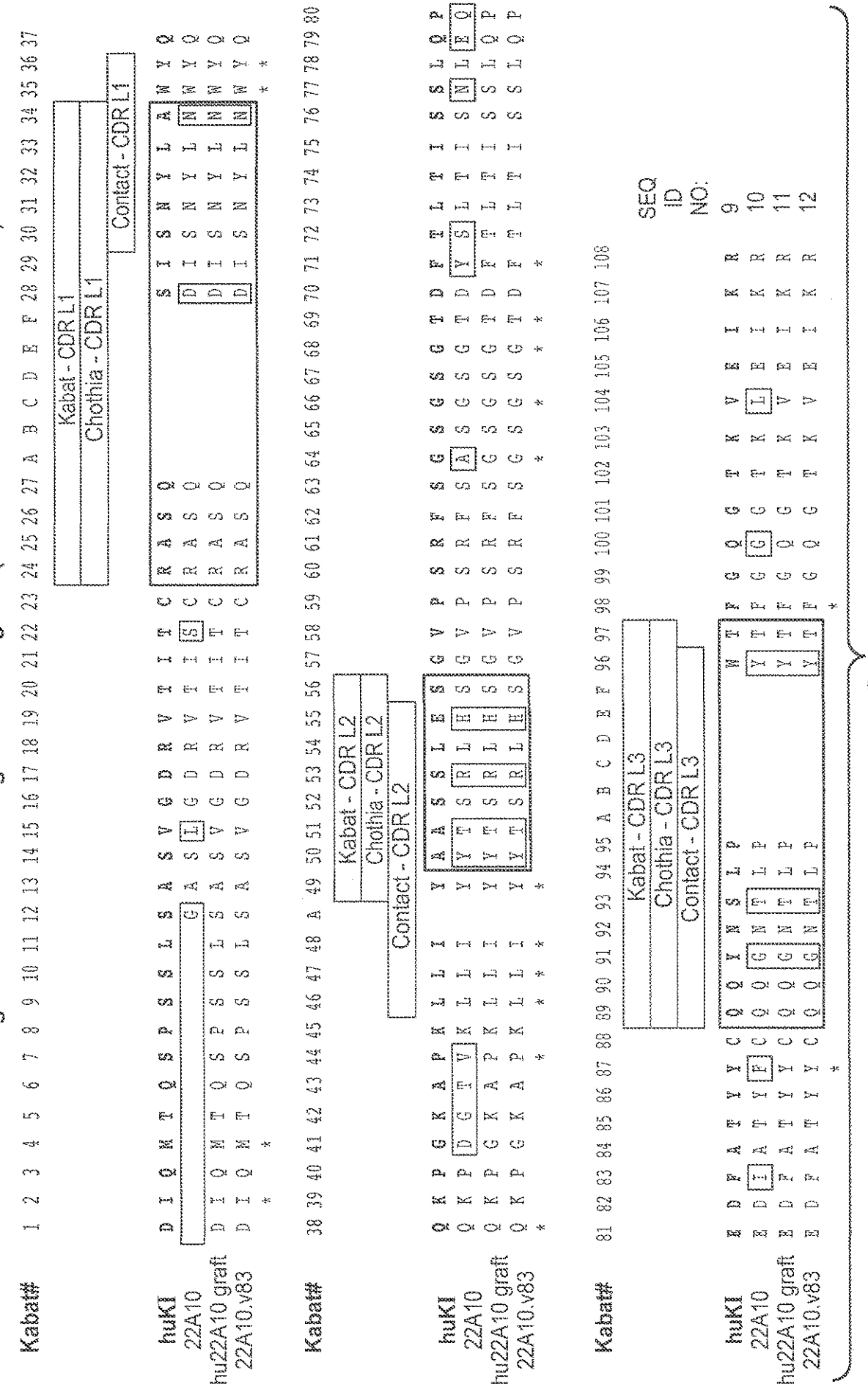

Alignment of Variable Light Chain Regions (Murine and Humanized 22A10)
Kabat - CDR L1
Chothia - CDR L1
Contact - CDR L1
Kabat - CDR L2
Chothia - CDR L2
Contact - CDR L2
Kabat - CDR L3
Chothia - CDR L3
Contact - CDR L3
SEQ ID NO:
9
10
11
12

FIG. 7

Alignment of Variable Heavy Chain Regions (Murine and Humanized 22A10)

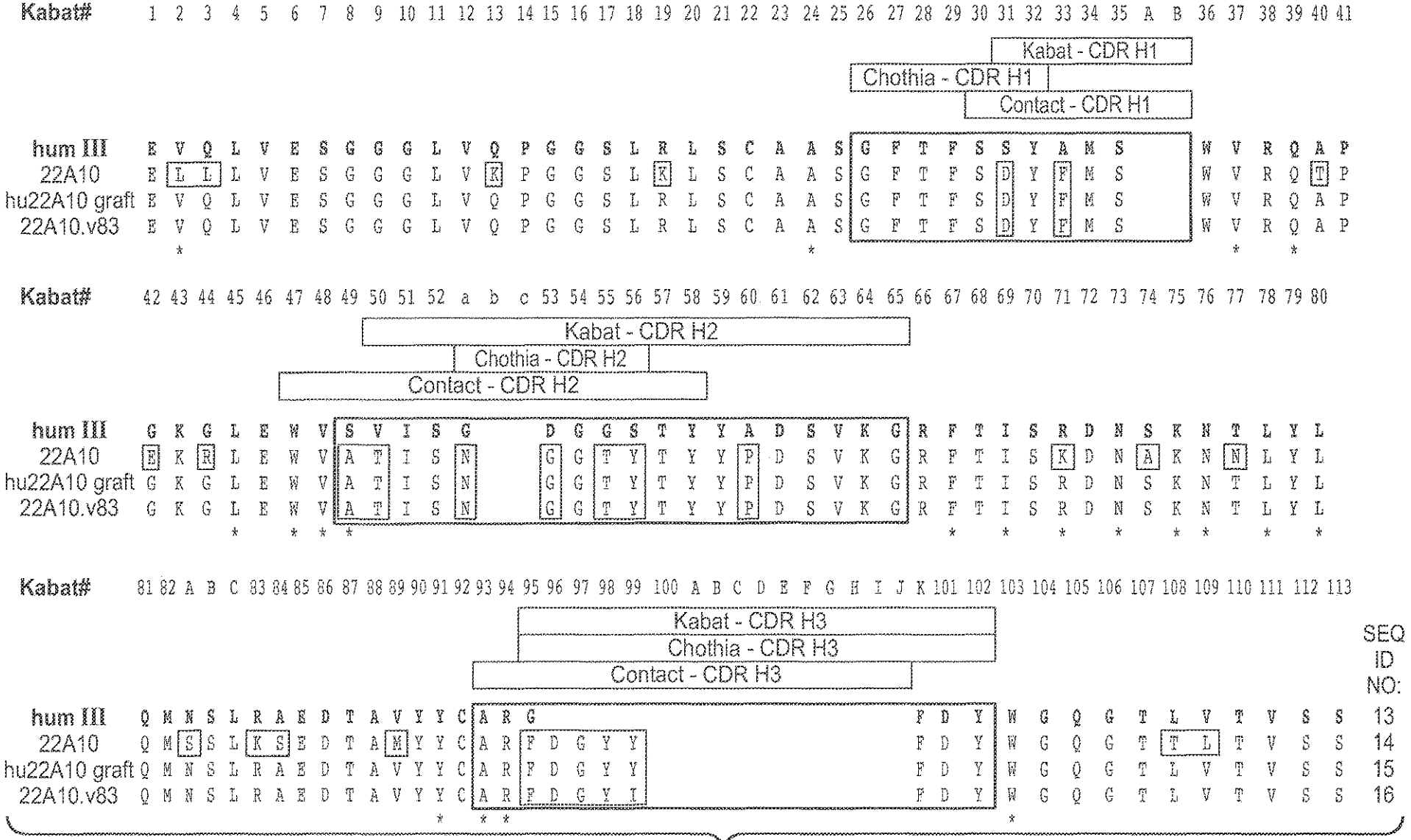


FIG. 8

Scatchard Analysis of Humanized 22A10 Variants on gD-Mesothelin BJAB Stable Cells

Panned On	-		Cyno		Cyno+Hu		Cyno	
h22A10 Version	Graft nM	Graft Sites	v1 nM	v1 Sites	v17 nM	v17 Sites	v83 nM	v83 Sites
Cyno BJAB	1.0	25000	1.0	21000	1.0	25000	1.3	45000
Human BJAB	1.6	18000	1.9	16000	1.7	17000	1.8	31000
Rat BJAB	1.9	22400	2.8	15000	3.9	24000	2.7	31000

FIG. 9A

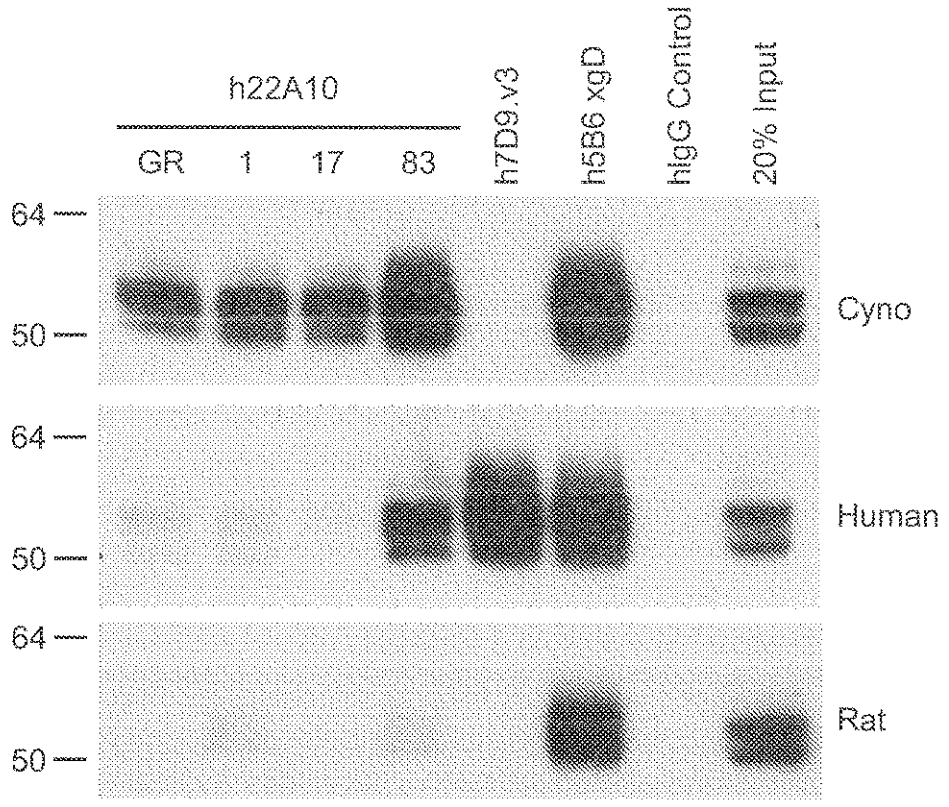


FIG. 9B

Humanized Antibody 7D9 Region	Sequence	SEQ ID NO:
h7D9.v1, h7D9.v3 HVR-L1	KSSQSVLYSSNQKNYLA	17
h7D9.v1, h7D9.v3 HVR-L2	WASTRES	18
h7D9.v1, h7D9.v3 HVR-L3	HQYLSSYT	19
h7D9.v1, h7D9.v3 HVR-H1	GYTFTTYWMH	20
h7D9.v1, h7D9.v3 HVR-H2	GYIRPSTGYTEYNQKFKD	21
h7D9.v1, h7D9.v3 HVR-H3	ARSRWLLDY	22
h7D9.v1, h7D9.v3 VL-FR1	DIQMTQSPSSLSASVGDRVTITC	23
h7D9.v1 VL-FR2	WYQQKPGKAPKLLIY	24
h7D9.v3 VL-FR2	WFQQKPGKAPKLLIY	25
h7D9.v1 VL-FR3	GVPSRFSGSGSGTDFTLTISSLQPEDFATYYC	26
h7D9.v3 VL-FR3	GVPSRFSGSGSGTDFTLTISSLQPEDFATYFC	27
h7D9.v1, h7D9.v3 VL-FR4	FGQGTKVEIKR	28
h7D9.v1, h7D9.v3 VH-FR1	EVQLVESGGGLVQPGGSLRLSCAAS	29
h7D9.v1, h7D9.v3 VH-FR2	WVRQAPGKGLEWV	30
h7D9.v1, h7D9.v3 VH-FR3	RFTISADTSKNTAYLQMNSLRAEDTAVYYC	31
h7D9.v1, h7D9.v3 VH-FR4	WGQGTLVTVS	32

FIG. 10A

Humanized Antibody 22A10 Region	Sequence	SEQ ID NO:
h22A10graft, h22A10.v83 HVR-L1	RASQDISNYLN	33
h22A10graft, h22A10v.83 HVR-L2	YTSRLHS	34
h22A10graft, h22A10v.83 HVR-L3	QQGNTLPYT	35
h22A10graft, h22A10v.83 HVR-H1	GFTFSDYFMS	36
h22A10graft, h22A10v.83 HVR-H2	ATISNGGTYTYYPDSVKG	37
h22A10graft HVR-H3	ARFDGYYFDY	38
h22A10v.83 HVR-H3	ARFDGYIFDY	39
h22A10graft, h22A10.v83 VL-FR1	DIQMTQSPSSLSASVGDRVTITC	23
h22A10graft, h22A10.v83 VL-FR2	WYQQKPGKAPKLLIY	24
h22A10graft, h22A10.v83 VL-FR3	GVPSRFSGSGSGTDFTLTISSLQPEDFATYYC	26
h22A10graft, h22A10.v83 VL-FR4	FGQGTKVEIKR	28
h22A10graft, h22A10.v83 VH-FR1	EVQLVESGGGLVQPGGSLRLSCAAS	29
h22A10graft, h22A10.v83 VH-FR2	WVRQAPGKGLEWV	30
h22A10graft, h22A10.v83 VH-FR3	RFTISRDNSKNTLYLQMNSLRAEDTAVYYC	40
h22A10graft, h22A10.v83 VH-FR4	WGQGTLVTVSS	41

FIG. 10B

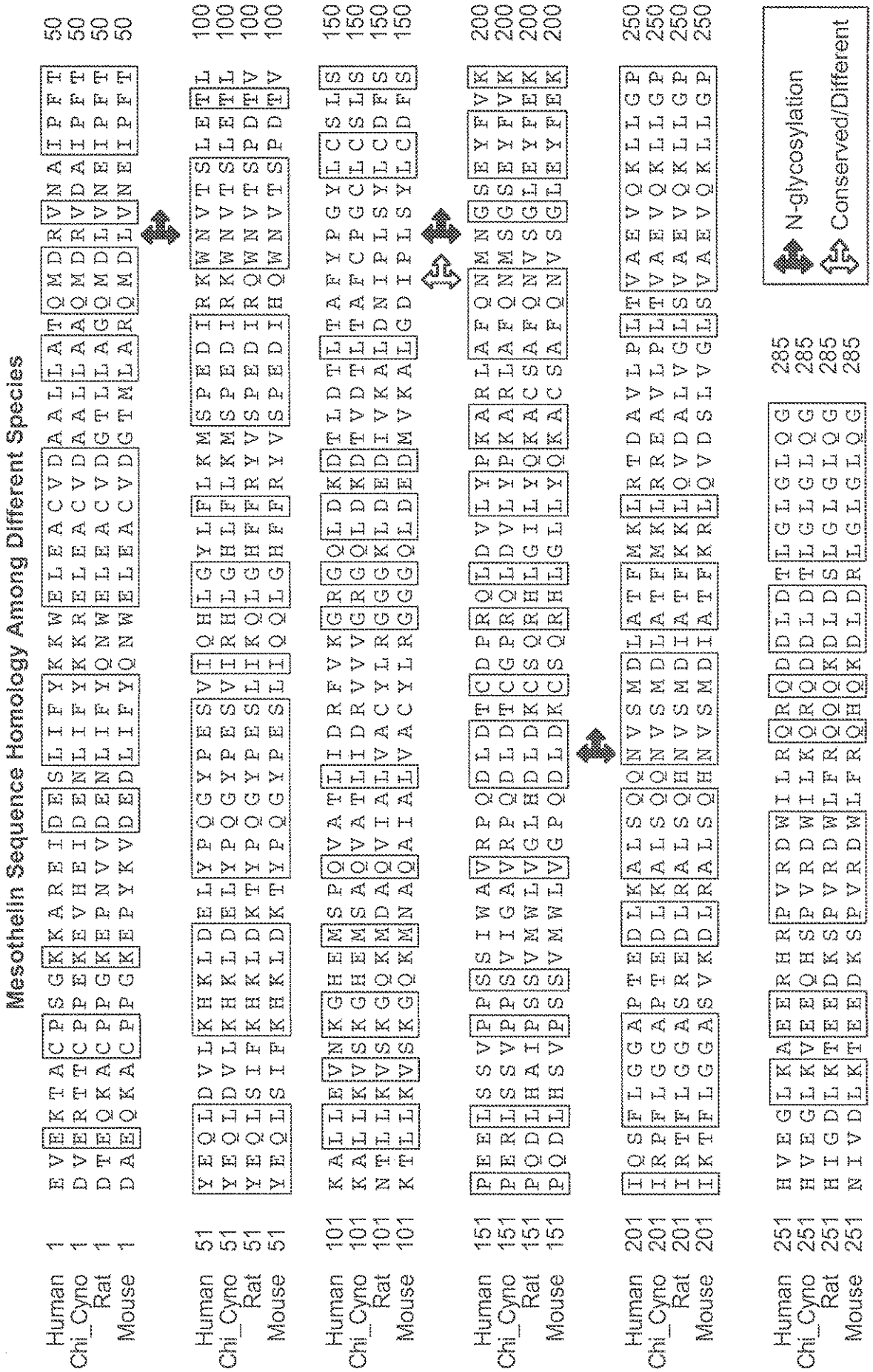

Mesothelin Sequence Homology Among Different Species
Human 1 EVEKTACPSGKKARETIDESLIFYKKWELEACVDAALLATQMDRVNAIPFT 50
Chi_Cyno 1 DVERTTCPPEKEVHEIDENLIFYKKRELEACVDAALLAAQMDRVDAIPFT 50
Rat 1 DTEQKACPPGKEPNVVDENLIFYQNWELEACVDGTLLAGQMDLVNEIPFT 50
Mouse 1 DAEQKACPPGKEPYKVDENLIFYQNWELEACVDGTMLARQMDLVNEIPFT 50
Human 51 YEQLDVLKHKLDELYPQGYPESVIQHLGYLFLKMSPEDIRKWNVTSLETL 100
Chi_Cyno 51 YEQLDVLKHKLDELYPQGYPESVIHRHLGHLFLKMSPEDIRKWNVTSLETL 100
Rat 51 YEQLSIFKHKLDKTYPQGYPESLIHQQLGHFRYVSPEDIRQWNVTSPDTV 100
Mouse 51 YEQLSIFKHKLDKTYPQGYPESLIQQLGHFRYVSPEDIHQWNVTSPDTV 100
Human 101 KALLEVNKGHEMSPQVATLIDRFVKGRGQLDKDTLDTLTAFYPGYLCSLS 150
Chi_Cyno 101 KALLKVSKGHEMSAQVATLIDRVVVGRGQLDKDTVDTLTAFCPGCLCSLS 150
Rat 101 NTLLKVSKGQKMDAQVIALVACYLRGGGKLDEDIVKALLDNIPLSYLCDFS 150
Mouse 101 KTLLKVSKGQKMNAQAIALVACYLRGGGQLDEDMVKALLGDIPLSYLCDFS 150
Human 151 PEELSSVPPSSIWAVRPQQDLDTCDPRQLDVLYPKARLAFQNMNGSEYFVK 200
Chi_Cyno 151 PERLSSVPPSSVIGAVRPQQDLDTCGPRQLDVLYPKARLAFQNMSGSEYFVK 200
Rat 151 PQDLHASVPSSVMWLVGLHDLDKCSQRHLGILYQKACSAFQNVSGLEYFEK 200
Mouse 151 PQDLHSVPSSVMWLVGPQQDLDKCSQRHLGLLYQKACSAFQNVSGLEYFEK 200
Human 201 HQSFLGGAPTEDLKALSQQNVSMDLATFMKLRTDAVLPLTVAEVQKLLGP 250
Chi_Cyno 201 IRPFLGGAPTEDLKALSQQNVSMDLATFMKLRREAVLPLTVAEVQKLLGP 250
Rat 201 HRTFLGGASREDLRALSQHNVSMDIATFFKKLQVDALVGLSVAEVQKLLGP 250
Mouse 201 HKTFLGGASVKDLRALSQHNVSMDIATFFKRLQVDSLVGLSVAEVQKLLGP 250
Human 251 HVEGLKAEERHRPVRDWILRQRQDDLDTLGLGLQG 285
Chi_Cyno 251 HVEGLKVEEQHSPVRDWILKQRQDDLDTLGLGLQG 285
Rat 251 HIGDLKTEEDKSPVRDWLFRQQQKDLDSLGLGLQG 285
Mouse 251 NIVDLKTEEDKSPVRDWLFRQHQKDLDRLGLGLQG 285
N-glycosylation
Conserved/Different

FIG. 11

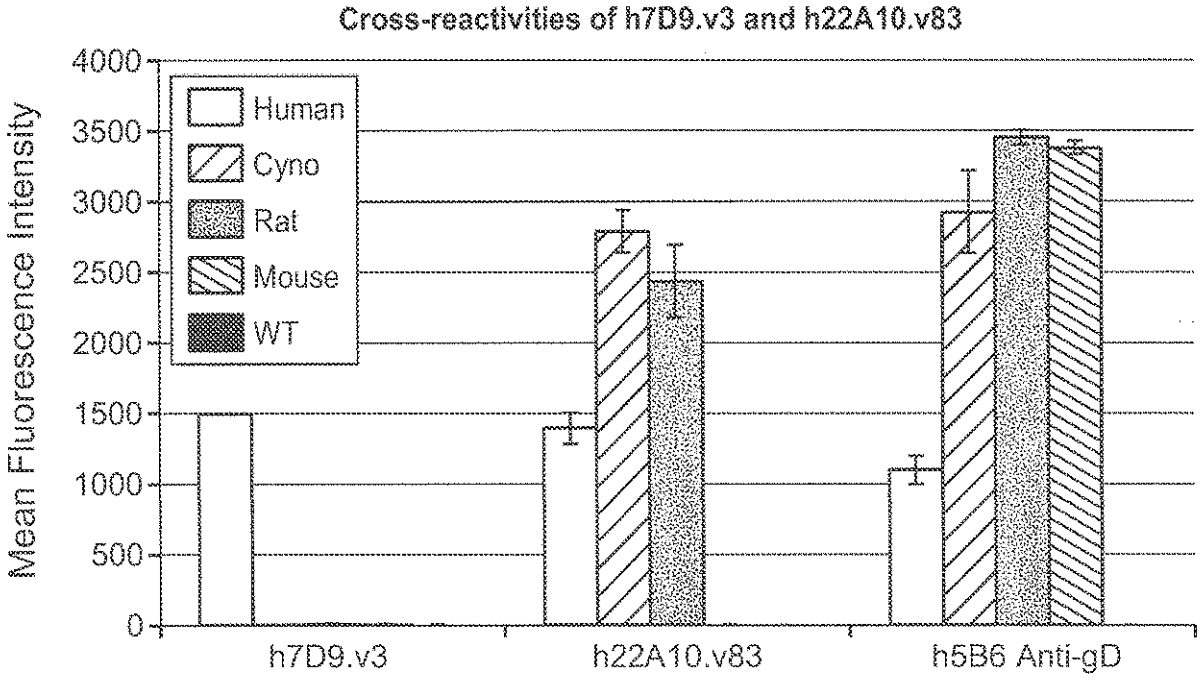


FIG. 12

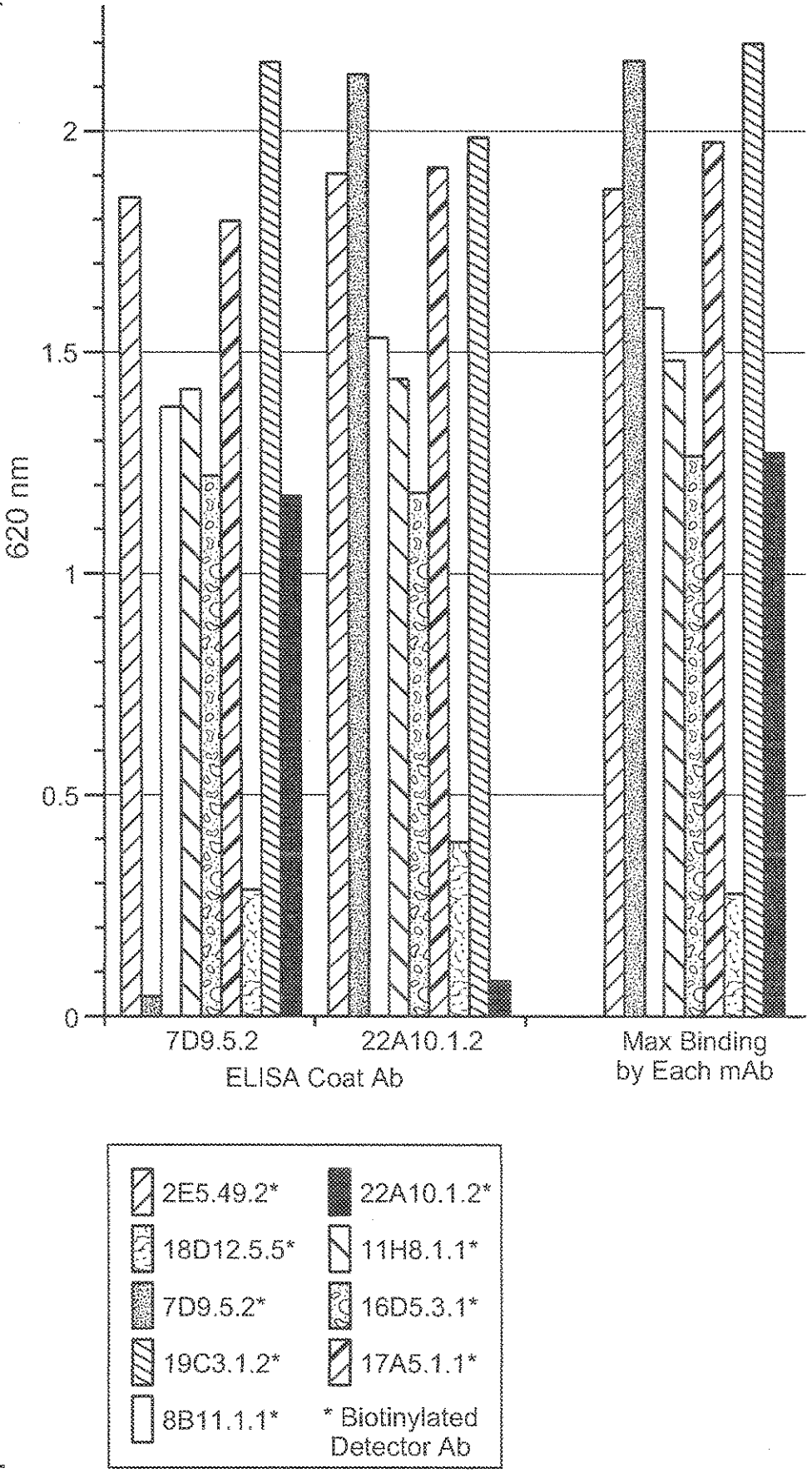
Anti-mesothelin Antibody Affinities

Scatchard Analysis on Mesothelin Stably Transfected and Endogenous Cell Lines:

	h7D9.v3 Kd (nM)	Copy #	h22A10.v83 Kd (nM)	Copy #
Human BJAB	**0.25**	20000	1.8	45000
Cyno BJAB	n.d.		**1.3**	31000
Rat BJAB	n.d.		2.7	31000
Human 293	**0.2**	n.d.	2.7	80500
Cyno 293	**n.b.**		**4.3**	356000
Rat 293	n.d.		7.3	81000
Human HT1080	**0.97**	130000	6.2	38000
Cyno HT1080	n.d.		**6.4**	113000
Rat 4/4-RM4	n.d.		6.2	171000
Endogenous				
OvCar3	0.53	14178	9.2	5516
OvCar3x2.1	0.56	39963	9	15294
HPAC	1	2600	9.4	7300
Capan2	0.63	10000	4.2	11250
AsPC1	0.58	2300	9.3	7100
HPAF-II	0.41	4200	10.45	6400

FIG. 13

FIG. 14


620 nm
2
1.5
1
0.5
0
7D9.5.2
22A10.1.2
Max Binding by Each mAb
ELISA Coat Ab
2E5.49.2*
18D12.5.5*
7D9.5.2*
19C3.1.2*
8B11.1.1*
22A10.1.2*
11H8.1.1*
16D5.3.1*
17A5.1.1*
* Biotinylated Detector Ab

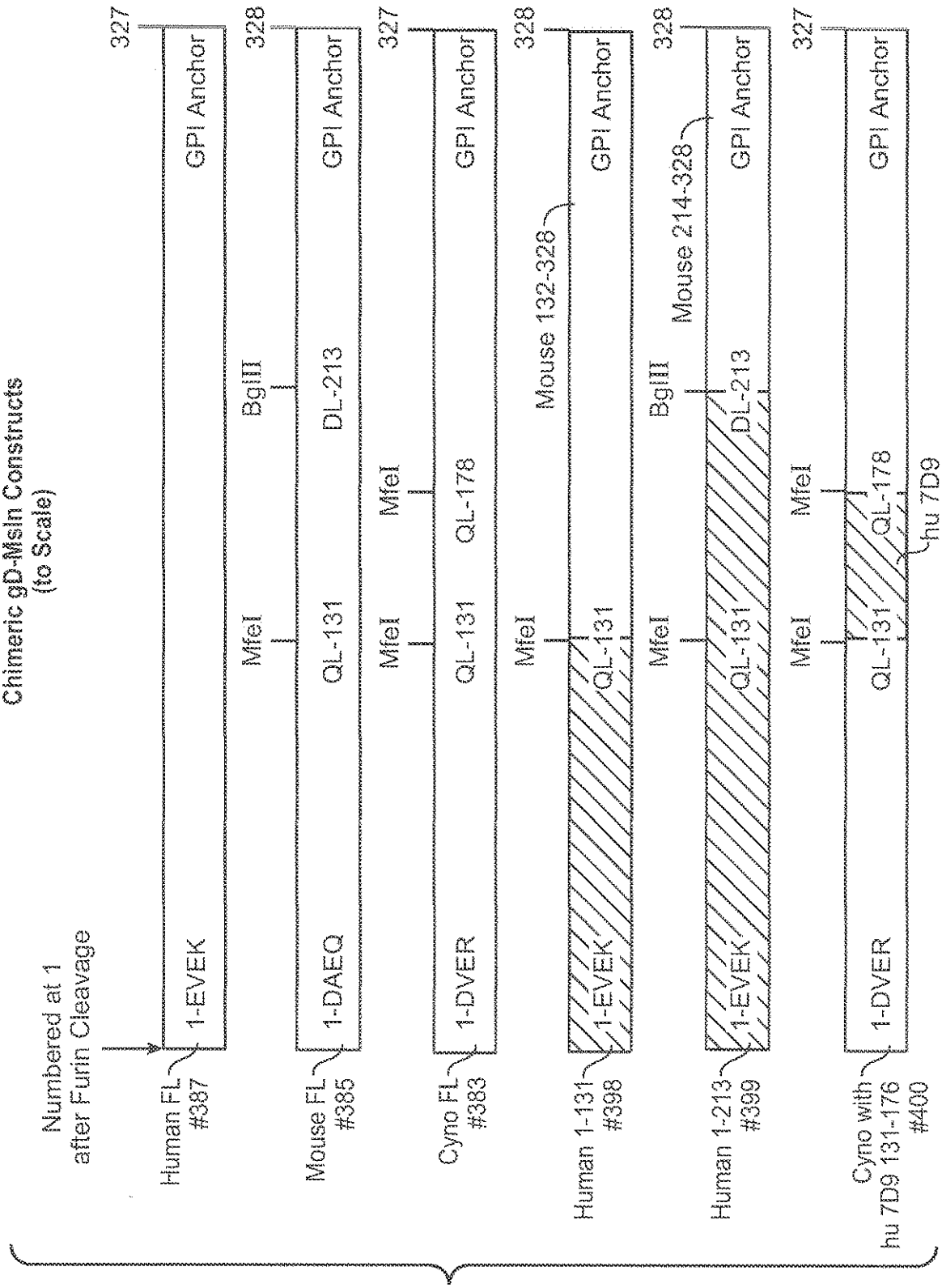

Chimeric gD-Msln Constructs
(to Scale)
Numbered at 1
after Furin Cleavage
327
328
327
328
328
327
GPI Anchor
BglII
MfeI
MfeI
MfeI
BglII
MfeI
Mouse 132-326
Mouse 214-328
DL-213
QL-131
QL-178
1-EVEK
1-DAEQ
1-DVER
Human FL
#387
Mouse FL
#385
Cyno FL
#383
Human 1-131
#398
Human 1-213
#399
Cyno with
hu 7D9 131-176
#400
hu 7D9

FIG. 15

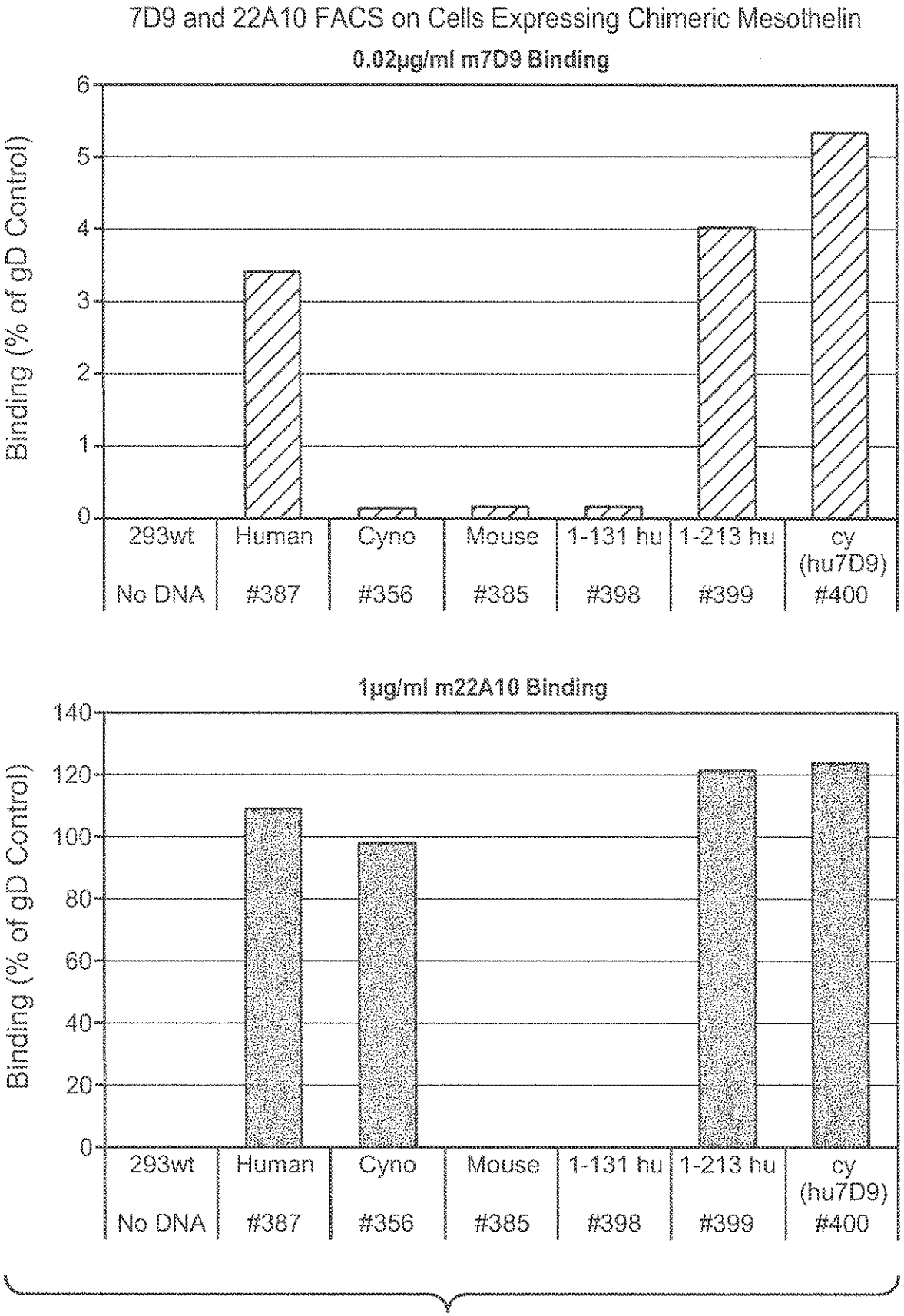
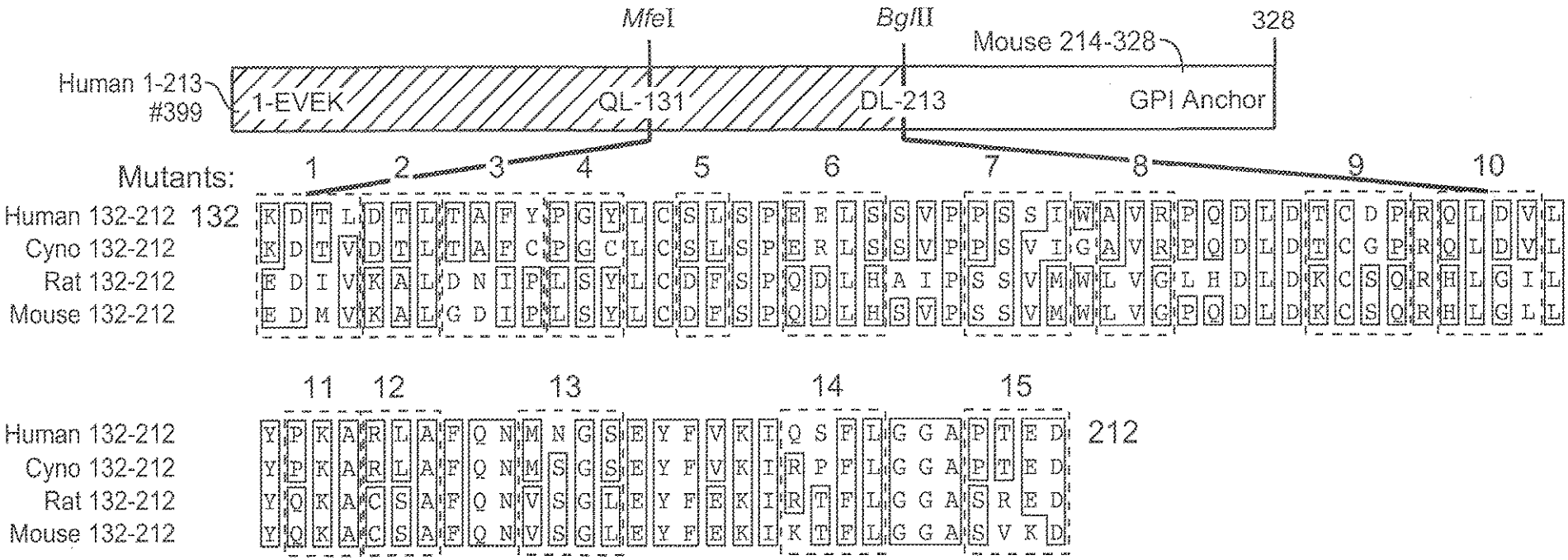

7D9 and 22A10 FACS on Cells Expressing Chimeric Mesothelin
0.02µg/ml m7D9 Binding
Binding (% of gD Control)
0
1
2
3
4
5
6
293wt
No DNA
Human
#387
Cyno
#356
Mouse
#385
1-131 hu
#398
1-213 hu
#399
cy
(hu7D9)
#400
1µg/ml m22A10 Binding
Binding (% of gD Control)
0
20
40
60
80
100
120
140
293wt
No DNA
Human
#387
Cyno
#356
Mouse
#385
1-131 hu
#398
1-213 hu
#399
cy
(hu7D9)
#400

FIG. 16



MUT1	**KDTL** EDMV	MUT6	**EELS** QDLH	MUT11	**PKA** QKA
MUT2	**DTL** KAL	MUT7	**PSSI** SSVM	MUT12	**RLA** CSA
MUT3	**TAFY** GDIP	MUT8	**AVR** LVG	MUT13	**MNGS** VSGL
MUT4	**PGY** LSY	MUT9	**TCDP** KCSQ	MUT14	**QSF** KTF
MUT5	**SL** DF	MUT10	**QLDVL** HLGLL	MUT15	**PTED** STKD (not SVKD)

15 human-to-mouse mutants were made between aa 132-212

The indicated **Human** seq was mutated to the indicated Mouse seq in each mutant

FIG. 17

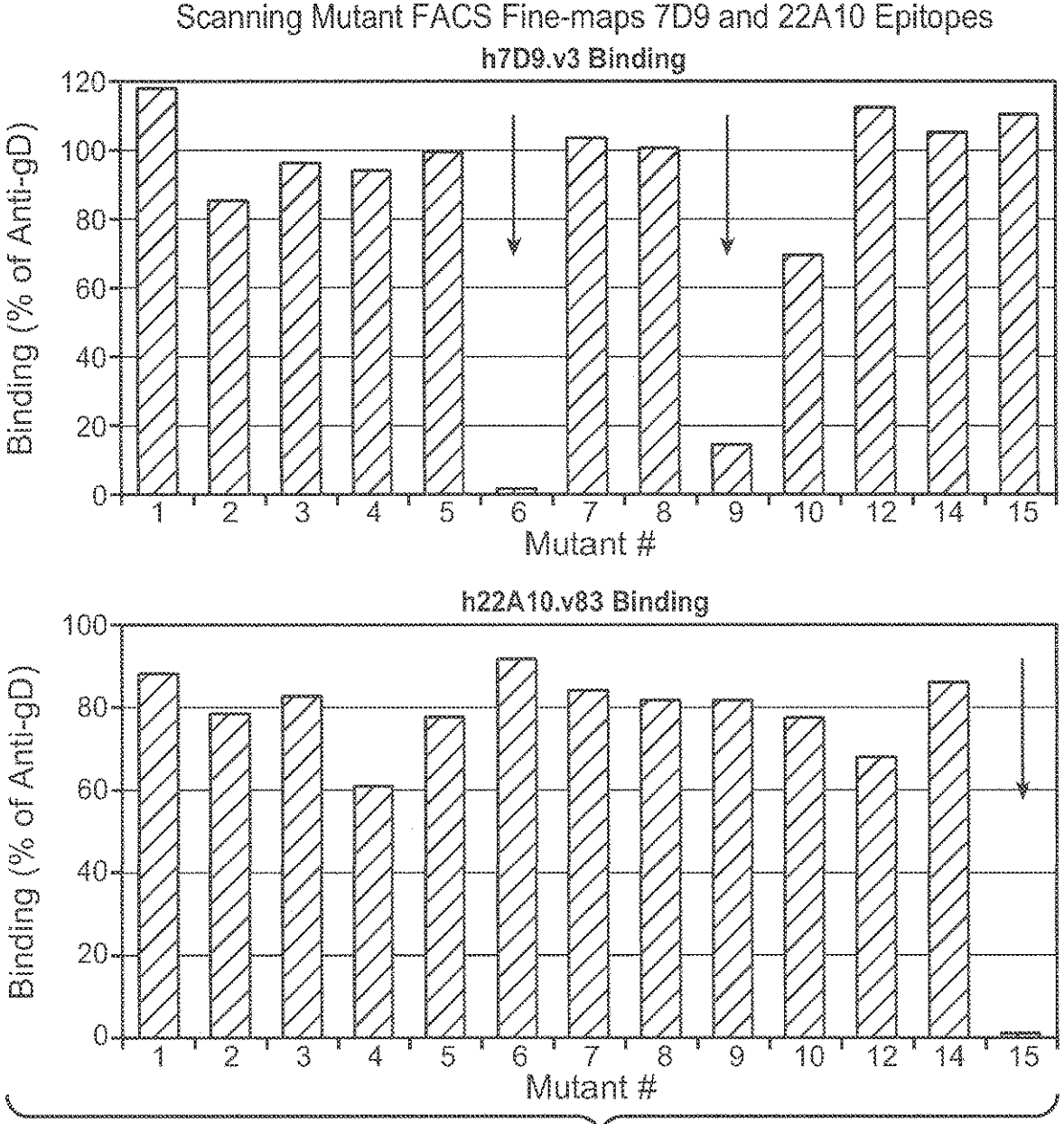


FIG. 18A

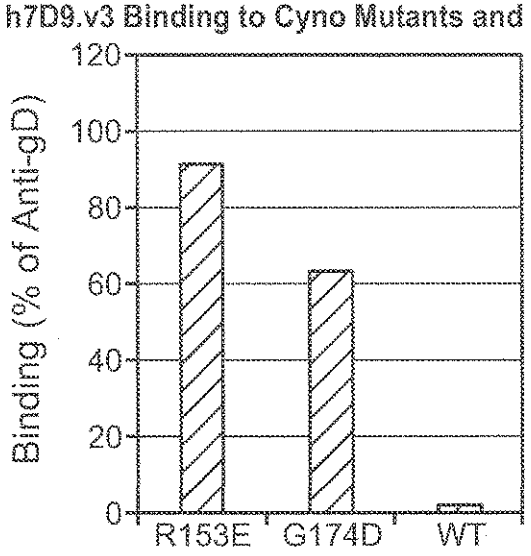


FIG. 18B

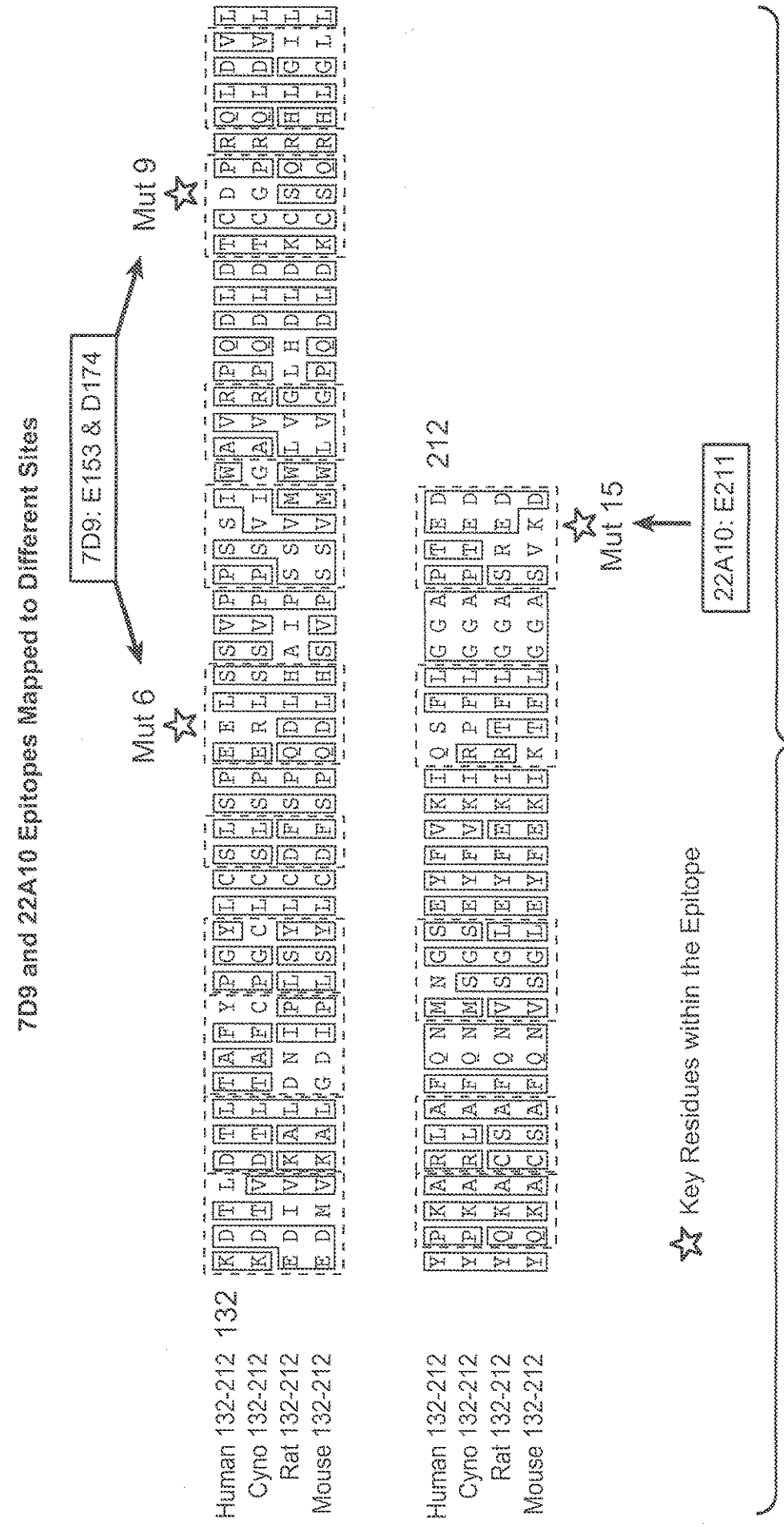
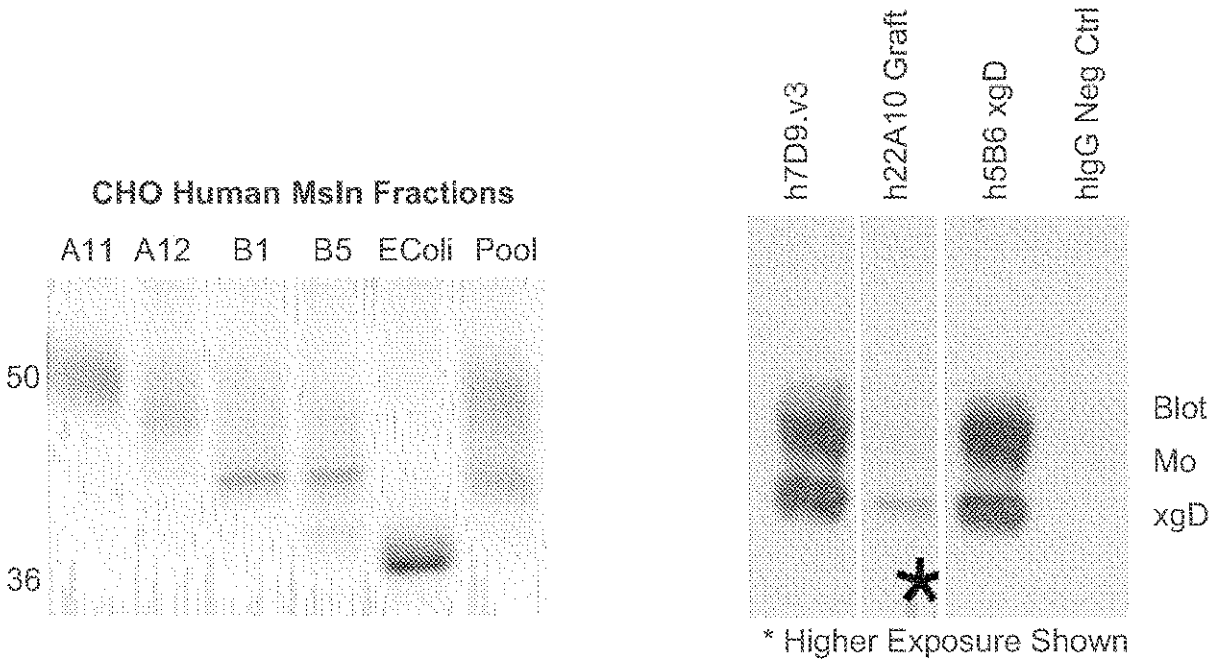

7D9 and 22A10 Epitopes Mapped to Different Sites
7D9: E153 & D174
Mut 6
Mut 9
Mut 15
22A10: E211
Key Residues within the Epitope
Human 132-212
Cyno 132-212
Rat 132-212
Mouse 132-212
132
212

FIG. 19


CHO Human MsIn Fractions
A11
A12
B1
B5
EColi
Pool
50
36
h7D9.v3
h22A10 Graft
h5B6 xgD
hIgG Neg Ctrl
Blot
Mo
xgD
* Higher Exposure Shown

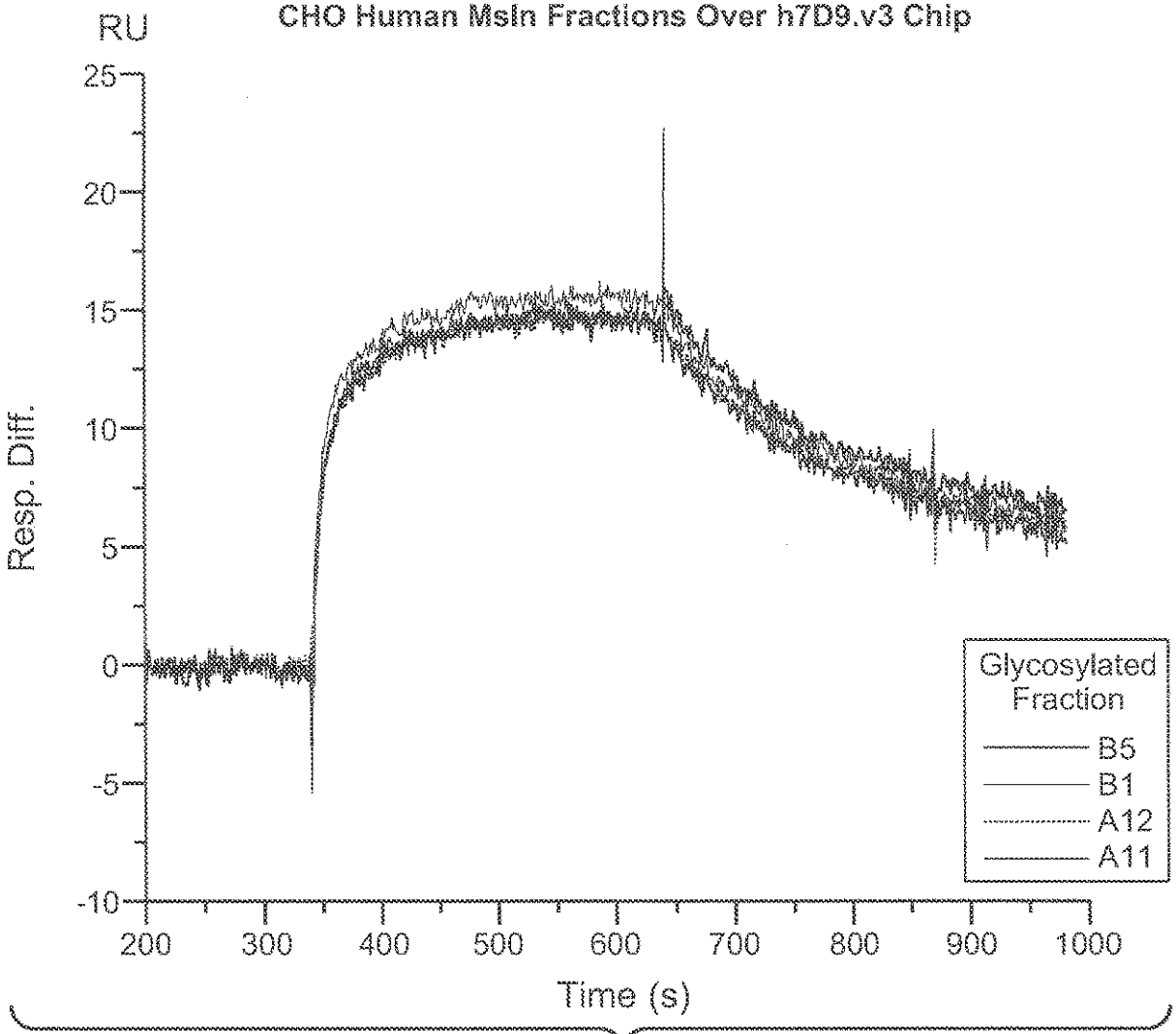
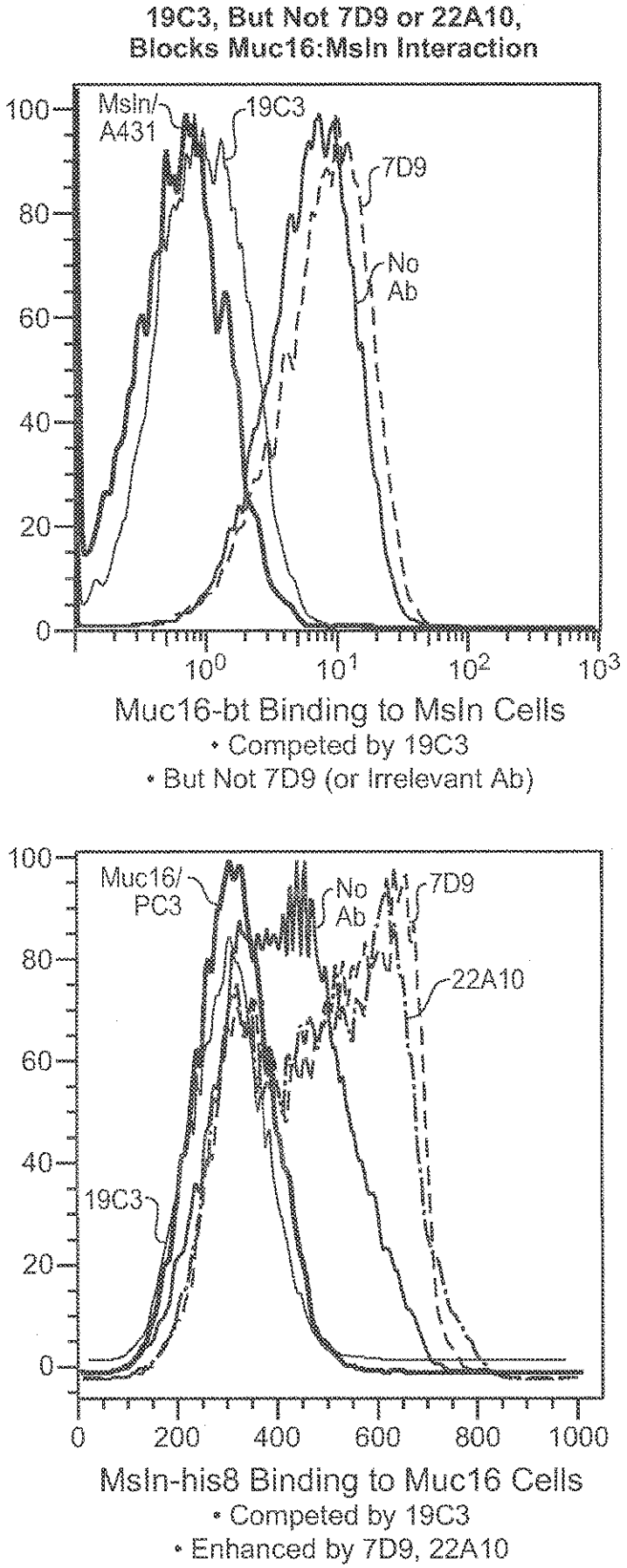

CHO Human MsIn Fractions Over h7D9.v3 Chip
RU
Resp. Diff.
25
20
15
10
5
0
-5
-10
200
300
400
500
600
700
800
900
1000
Time (s)
Glycosylated Fraction
B5
B1
A12
A11

FIG. 20

FIG. 21


19C3, But Not 7D9 or 22A10,
Blocks Muc16:MsIn Interaction
MsIn/
A431
19C3
7D9
No
Ab
100
80
60
40
20
0
10^0
10^1
10^2
10^3
Muc16-bt Binding to MsIn Cells
• Competed by 19C3
• But Not 7D9 (or Irrelevant Ab)
Muc16/
PC3
No
Ab
7D9
22A10
19C3
0
200
400
600
800
1000
MsIn-his8 Binding to Muc16 Cells
• Competed by 19C3
• Enhanced by 7D9, 22A10

Mesothelin IHC Pancreatic Ductal Adenocarcinoma (PDAC)

	IHC Score			
	0+	1+	2+	3+
PDAC (N=76)	30%	37%	24%	9%

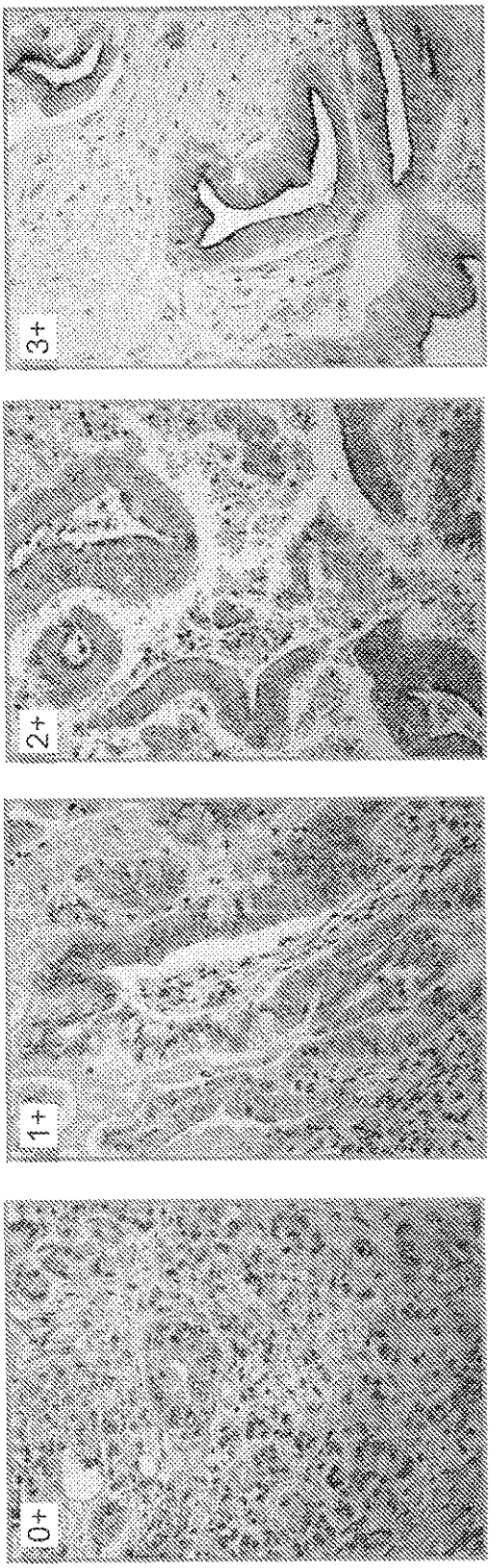
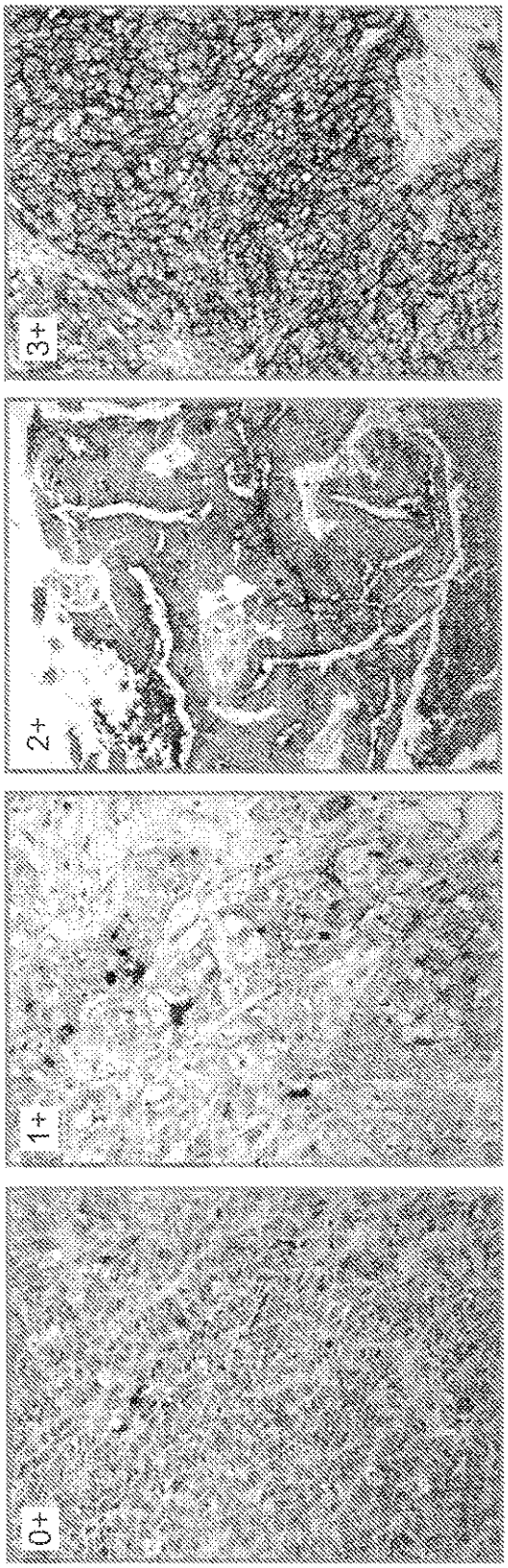


FIG. 22

Mesothelin IHC Ovarian Tumors

	IHC Score			
	0+	1+	2+	3+
Serous Adeno (N=43)	2%	23%	44%	30%



98% Serous Positive, 74% ≥ 2+. 8/8 Matched Serous Mets Positive

FIG. 23

Mesothelin IHC NSCLC Adenocarcinoma

	IHC Score			
	0+	1+	2+	3+
NSCLC (N=77)	56%	18%	16%	10%

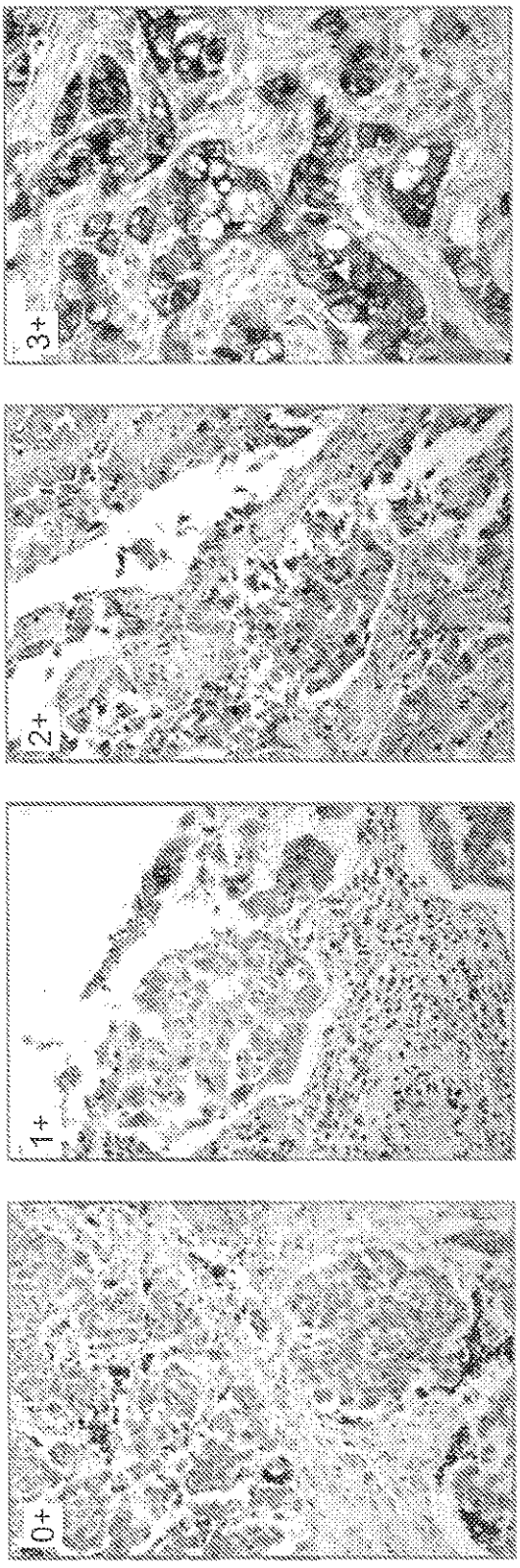


FIG. 24

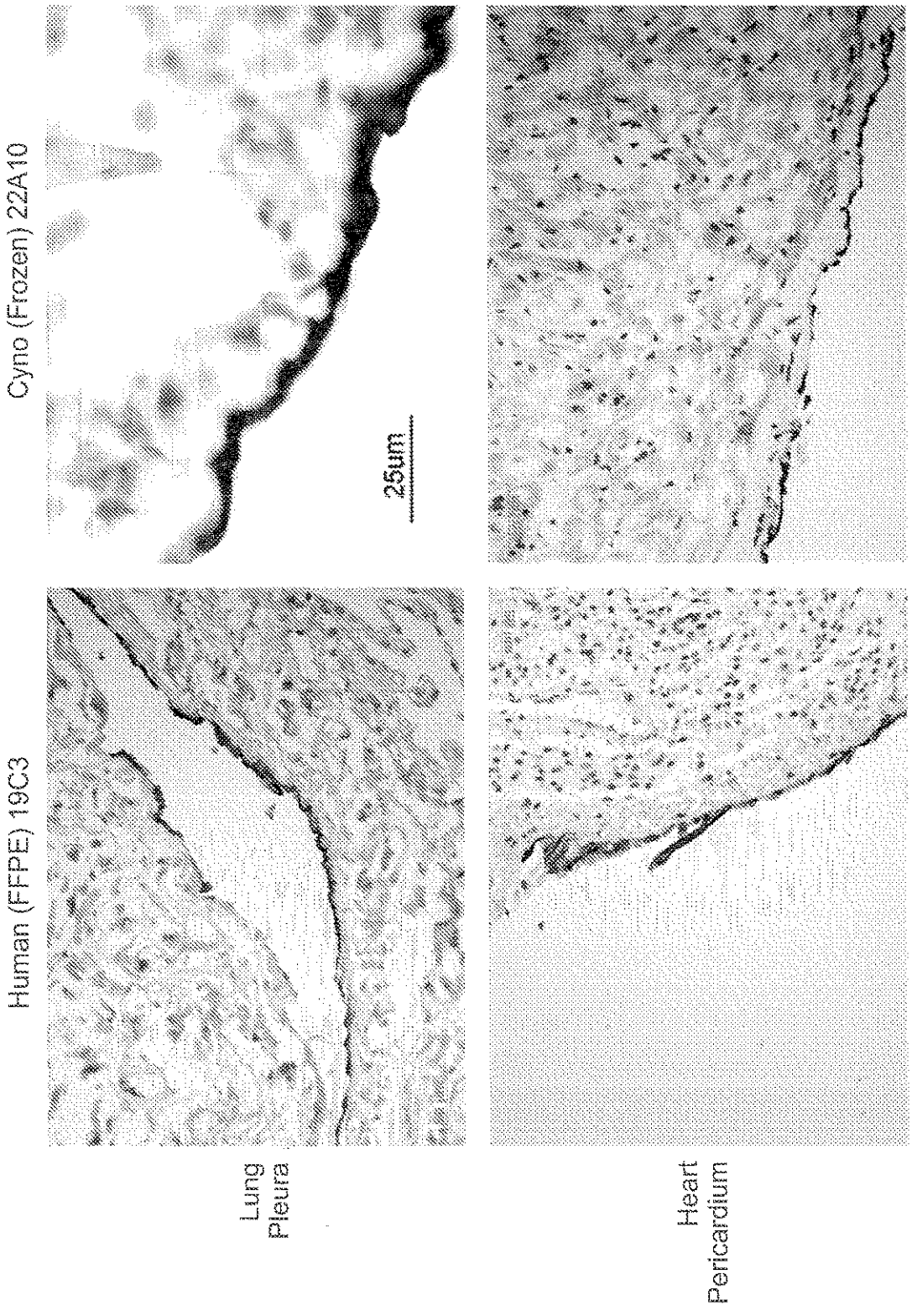

Human (FFPE) 19C3
Cyno (Frozen) 22A10
25um
Lung
Pleura
Heart
Pericardium
H2009-341
H2008-857-2

FIG. 25

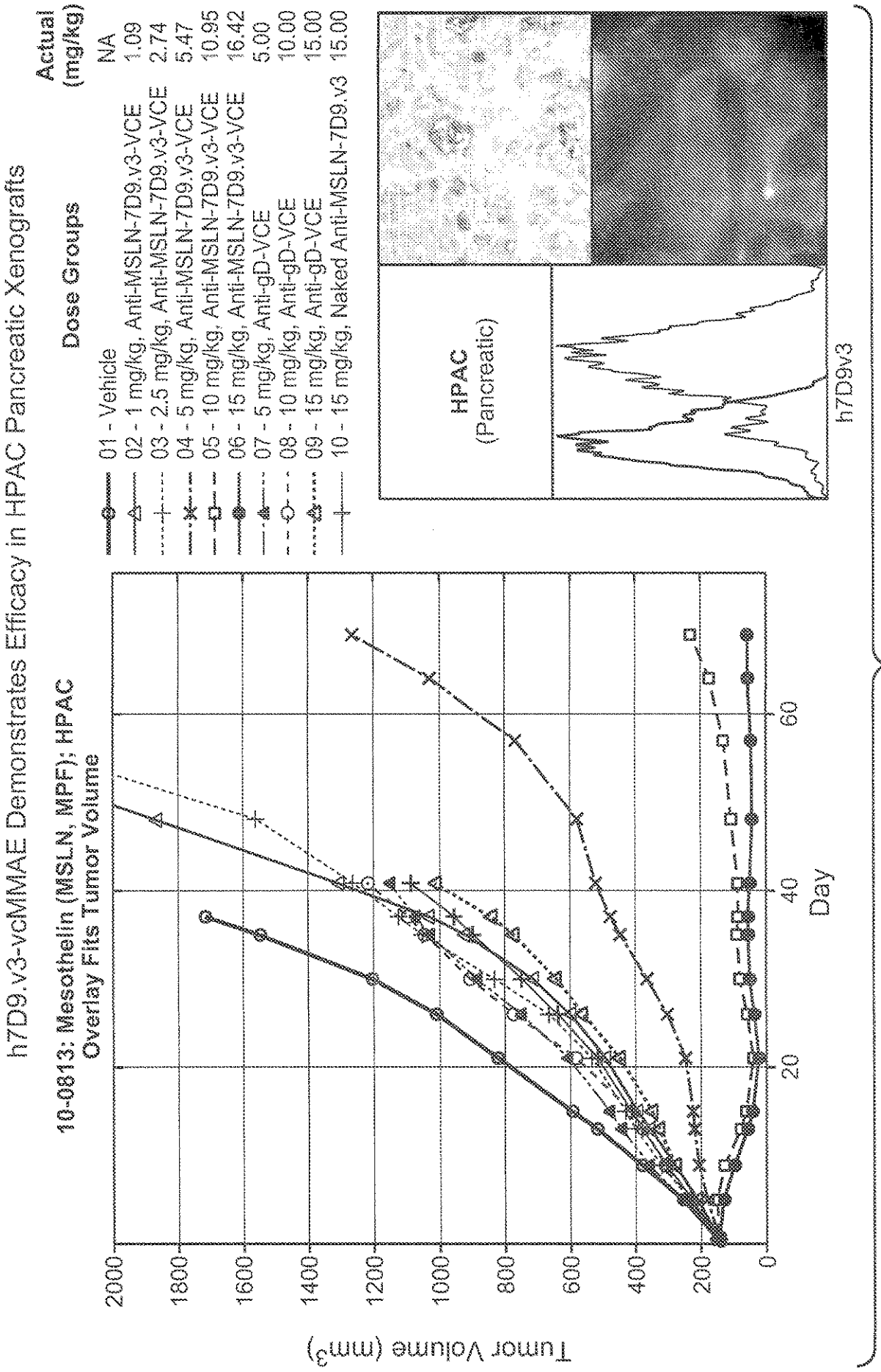

h7D9.v3-vcMMAE Demonstrates Efficacy in HPAC Pancreatic Xenografts
10-0813: Mesothelin (MSLN, MPF); HPAC
Overlay Fits Tumor Volume
Dose Groups
Actual (mg/kg)
01 - Vehicle NA
02 - 1 mg/kg, Anti-MSLN-7D9.v3-VCE 1.09
03 - 2.5 mg/kg, Anti-MSLN-7D9.v3-VCE 2.74
04 - 5 mg/kg, Anti-MSLN-7D9.v3-VCE 5.47
05 - 10 mg/kg, Anti-MSLN-7D9.v3-VCE 10.95
06 - 15 mg/kg, Anti-MSLN-7D9.v3-VCE 16.42
07 - 5 mg/kg, Anti-gD-VCE 5.00
08 - 10 mg/kg, Anti-gD-VCE 10.00
09 - 15 mg/kg, Anti-gD-VCE 15.00
10 - 15 mg/kg, Naked Anti-MSLN-7D9.v3 15.00
Tumor Volume (mm3)
2000
1800
1600
1400
1200
1000
800
600
400
200
0
20
40
60
Day
HPAC
(Pancreatic)
h7D9v3

FIG. 26

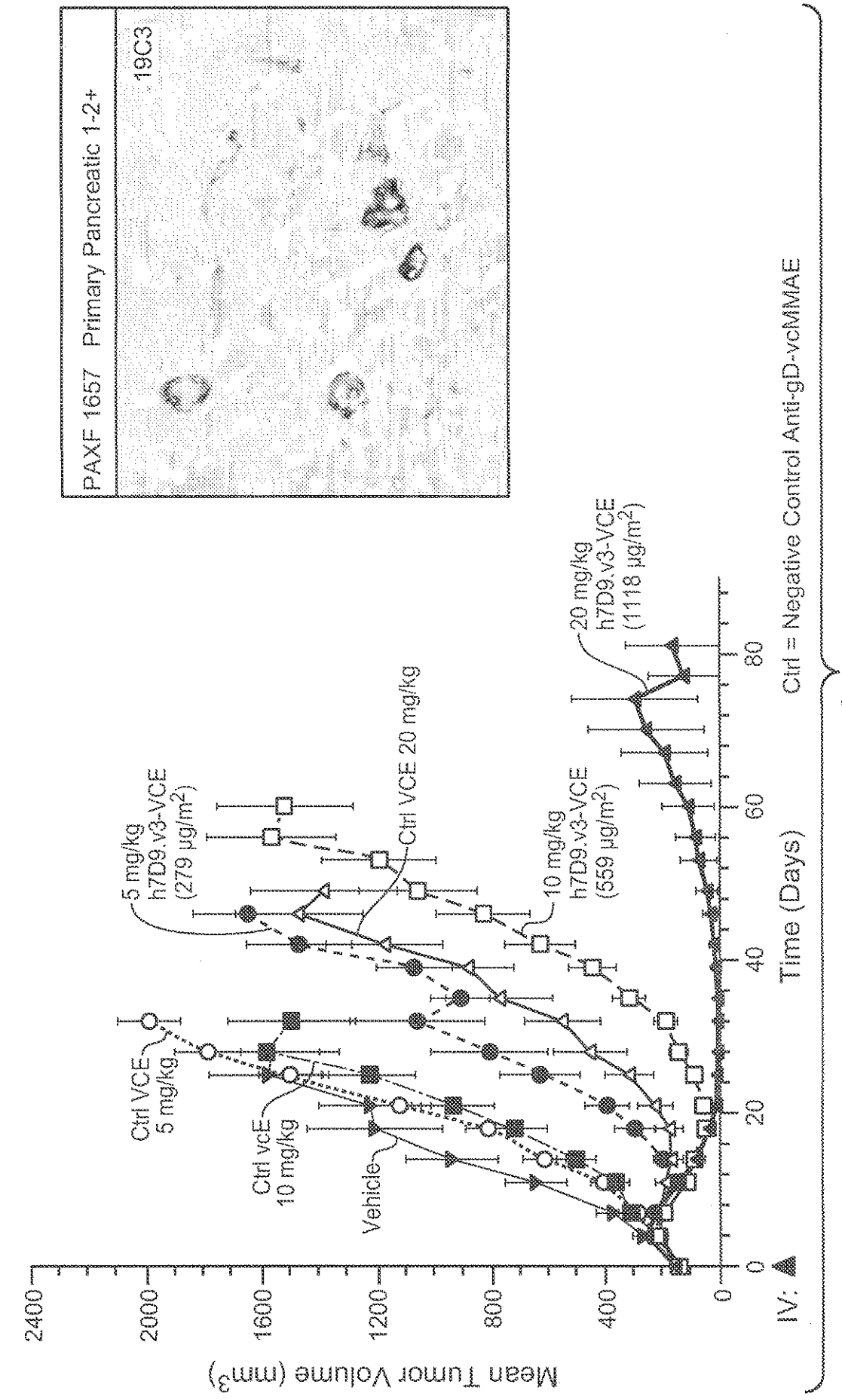

h7D9.v3-vcMMAE Demonstrates Efficacy in a Primary Pancreatic Xenograft
PAXF 1657 Primary Pancreatic 1-2+
19C3
Mean Tumor Volume (mm3)
2400
2000
1600
1200
800
400
0
0
20
40
60
80
Time (Days)
IV:
Ctrl VCE 5 mg/kg
Ctrl vcE 10 mg/kg
Vehicle
5 mg/kg h7D9.v3-VCE (279 µg/m2)
Ctrl VCE 20 mg/kg
10 mg/kg h7D9.v3-VCE (559 µg/m2)
20 mg/kg h7D9.v3-VCE (1118 µg/m2)
Ctrl = Negative Control Anti-gD-vcMMAE

FIG. 27

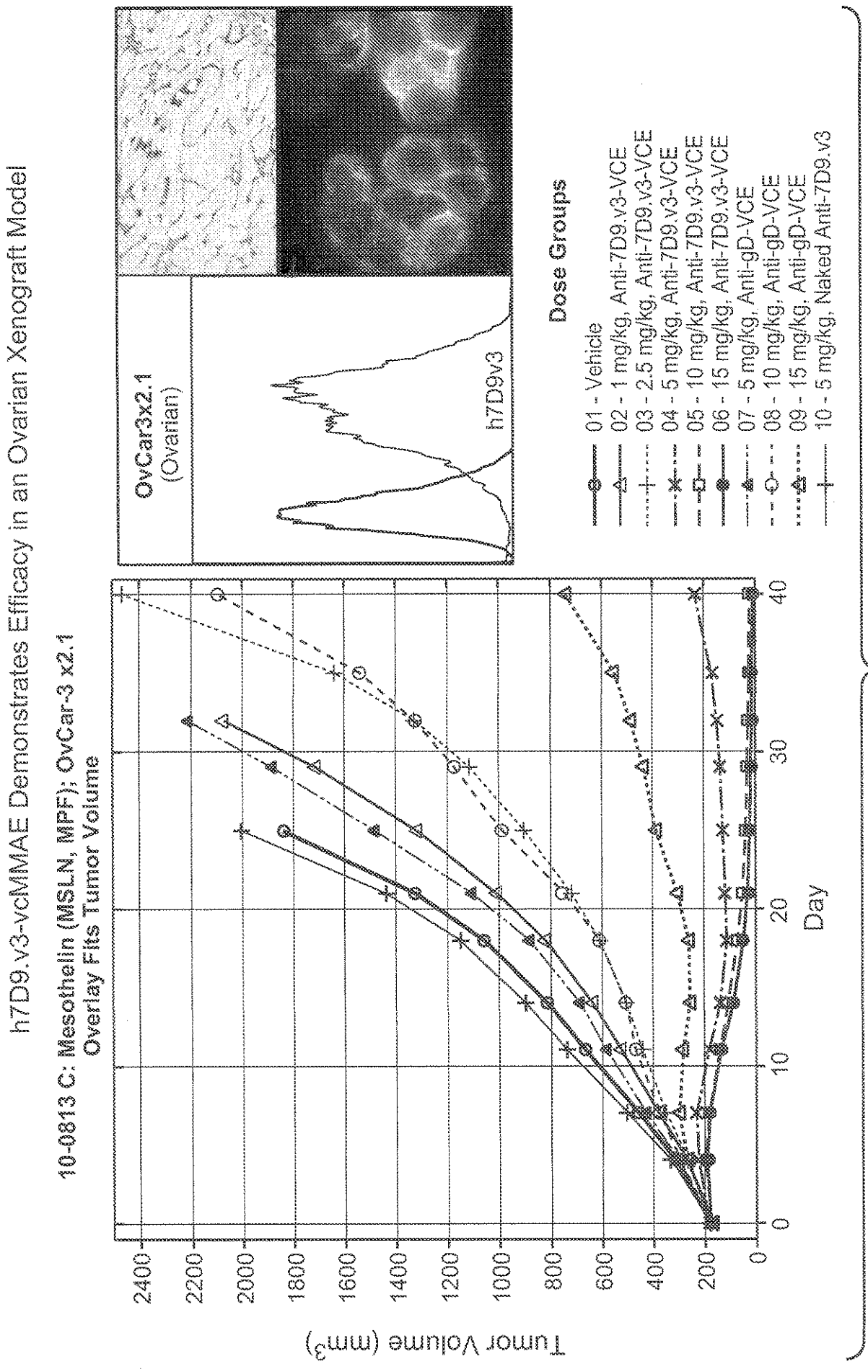

h7D9.v3-vcMMAE Demonstrates Efficacy in an Ovarian Xenograft Model
10-0813 C: Mesothelin (MSLN, MPF); OvCar-3 x2.1
Overlay Fits Tumor Volume
Tumor Volume (mm3)
Day
OvCar3x2.1
(Ovarian)
h7D9v3
Dose Groups
01 - Vehicle
02 - 1 mg/kg, Anti-7D9.v3-VCE
03 - 2.5 mg/kg, Anti-7D9.v3-VCE
04 - 5 mg/kg, Anti-7D9.v3-VCE
05 - 10 mg/kg, Anti-7D9.v3-VCE
06 - 15 mg/kg, Anti-7D9.v3-VCE
07 - 5 mg/kg, Anti-gD-VCE
08 - 10 mg/kg, Anti-gD-VCE
09 - 15 mg/kg, Anti-gD-VCE
10 - 5 mg/kg, Naked Anti-7D9.v3

FIG. 28

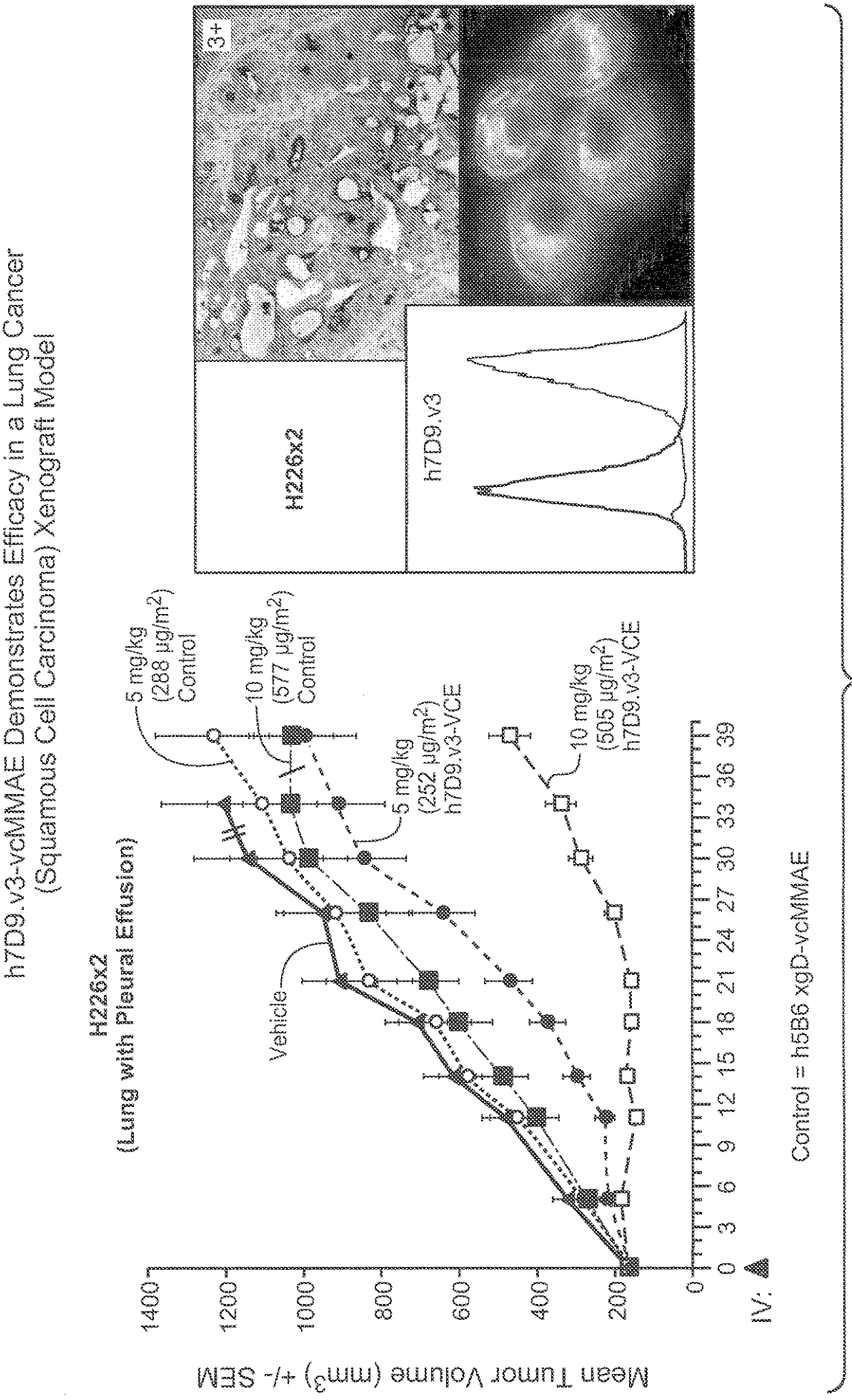

h7D9.v3-vcMMAE Demonstrates Efficacy in a Lung Cancer (Squamous Cell Carcinoma) Xenograft Model
H226x2 (Lung with Pleural Effusion)
Mean Tumor Volume (mm3) +/- SEM
1400
1200
1000
800
600
400
200
0
0 3 6 9 12 15 18 21 24 27 30 33 36 39
IV:
Vehicle
5 mg/kg (288 µg/m2) Control
10 mg/kg (577 µg/m2) Control
5 mg/kg (252 µg/m2) h7D9.v3-VCE
10 mg/kg (505 µg/m2) h7D9.v3-VCE
Control = h5B6 xgD-vcMMAE
H226x2
h7D9.v3
3+

FIG. 29

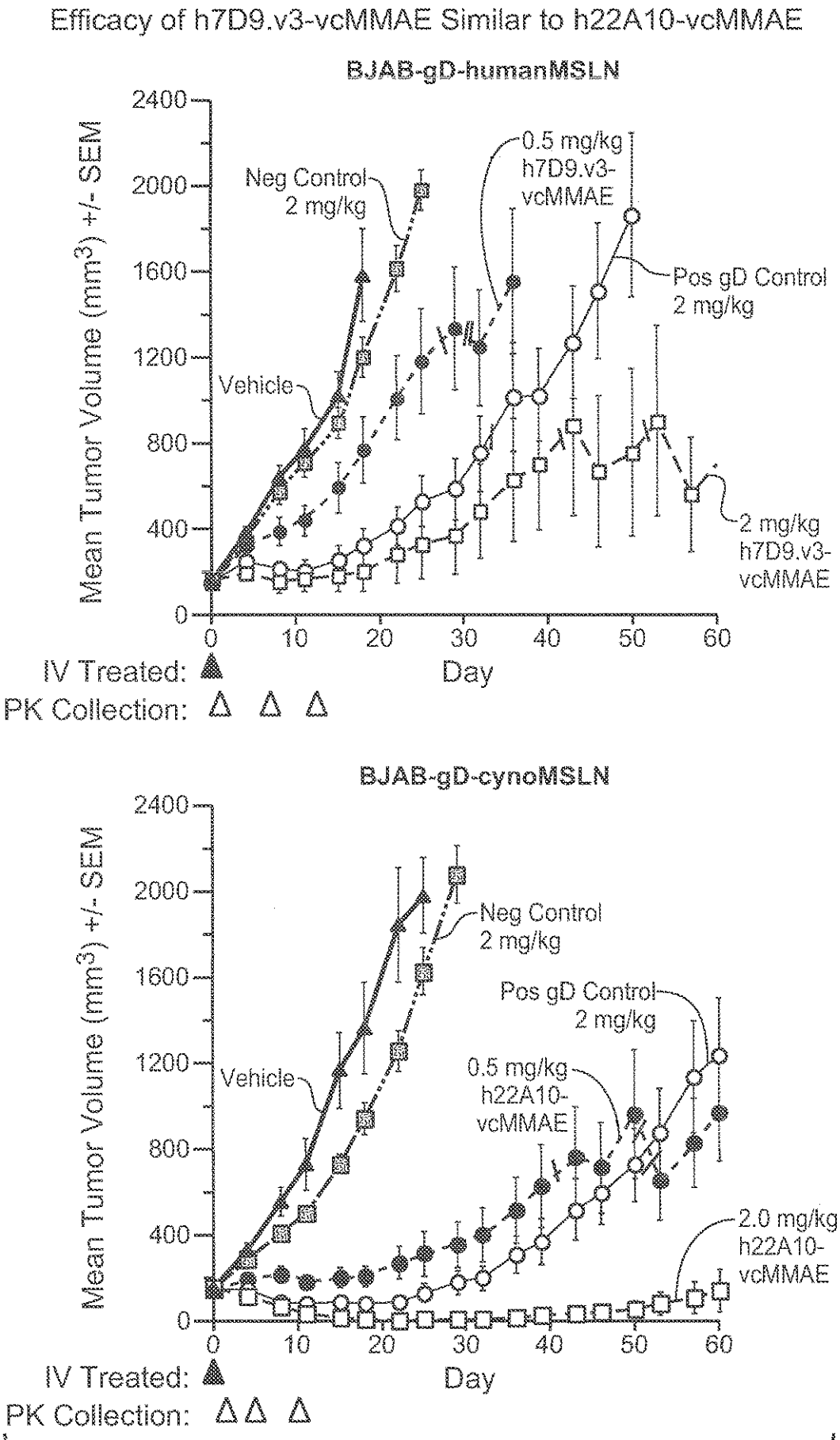

Efficacy of h7D9.v3-vcMMAE Similar to h22A10-vcMMAE
BJAB-gD-humanMSLN
Mean Tumor Volume (mm3) +/- SEM
2400
2000
1600
1200
800
400
0
Neg Control
2 mg/kg
0.5 mg/kg
h7D9.v3-
vcMMAE
Pos gD Control
2 mg/kg
Vehicle
2 mg/kg
h7D9.v3-
vcMMAE
0
10
20
30
40
50
60
Day
IV Treated:
PK Collection:
BJAB-gD-cynoMSLN
Mean Tumor Volume (mm3) +/- SEM
Neg Control
2 mg/kg
Pos gD Control
2 mg/kg
Vehicle
0.5 mg/kg
h22A10-
vcMMAE
2.0 mg/kg
h22A10-
vcMMAE
Day
IV Treated:
PK Collection:

FIG. 30

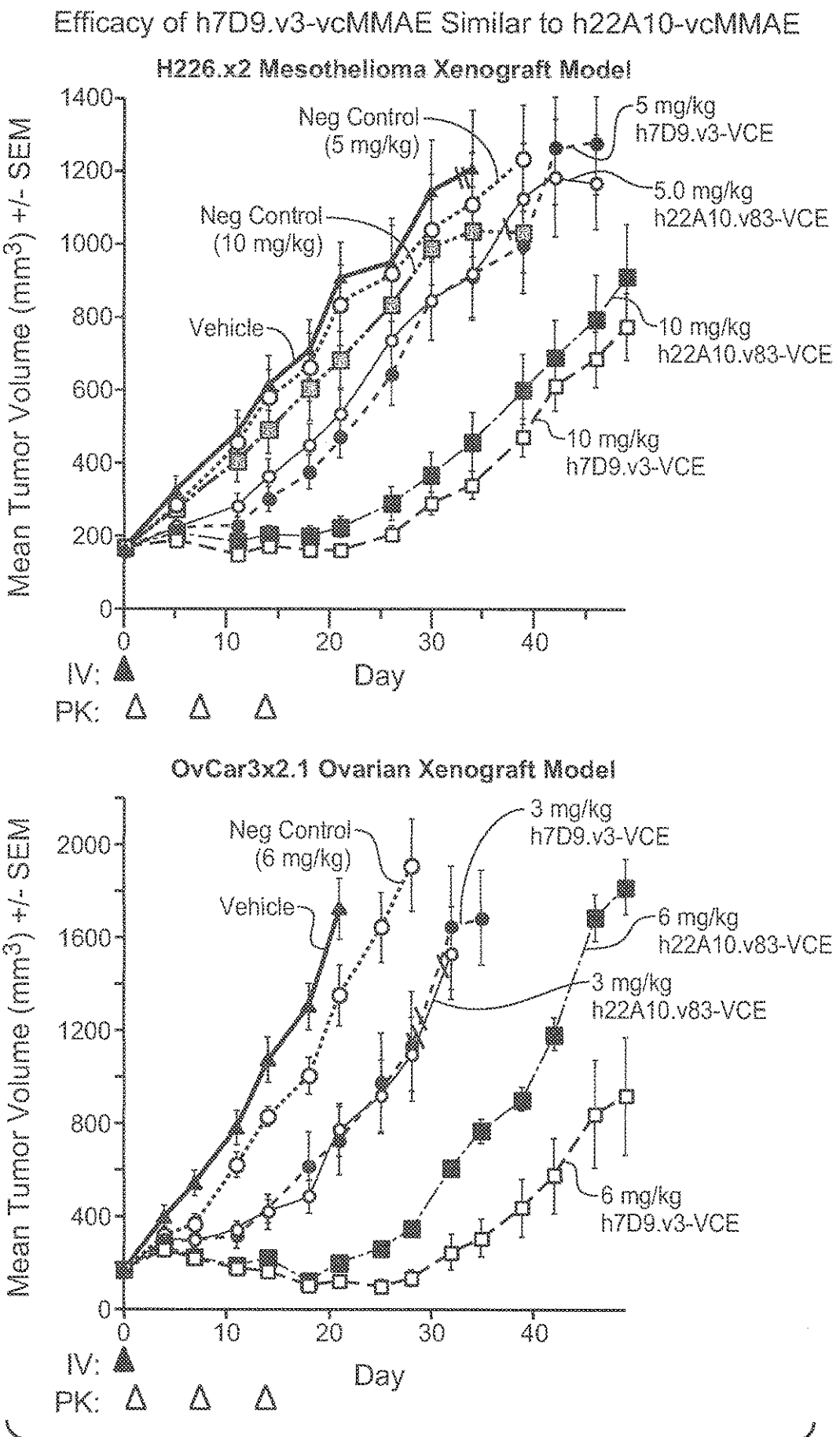
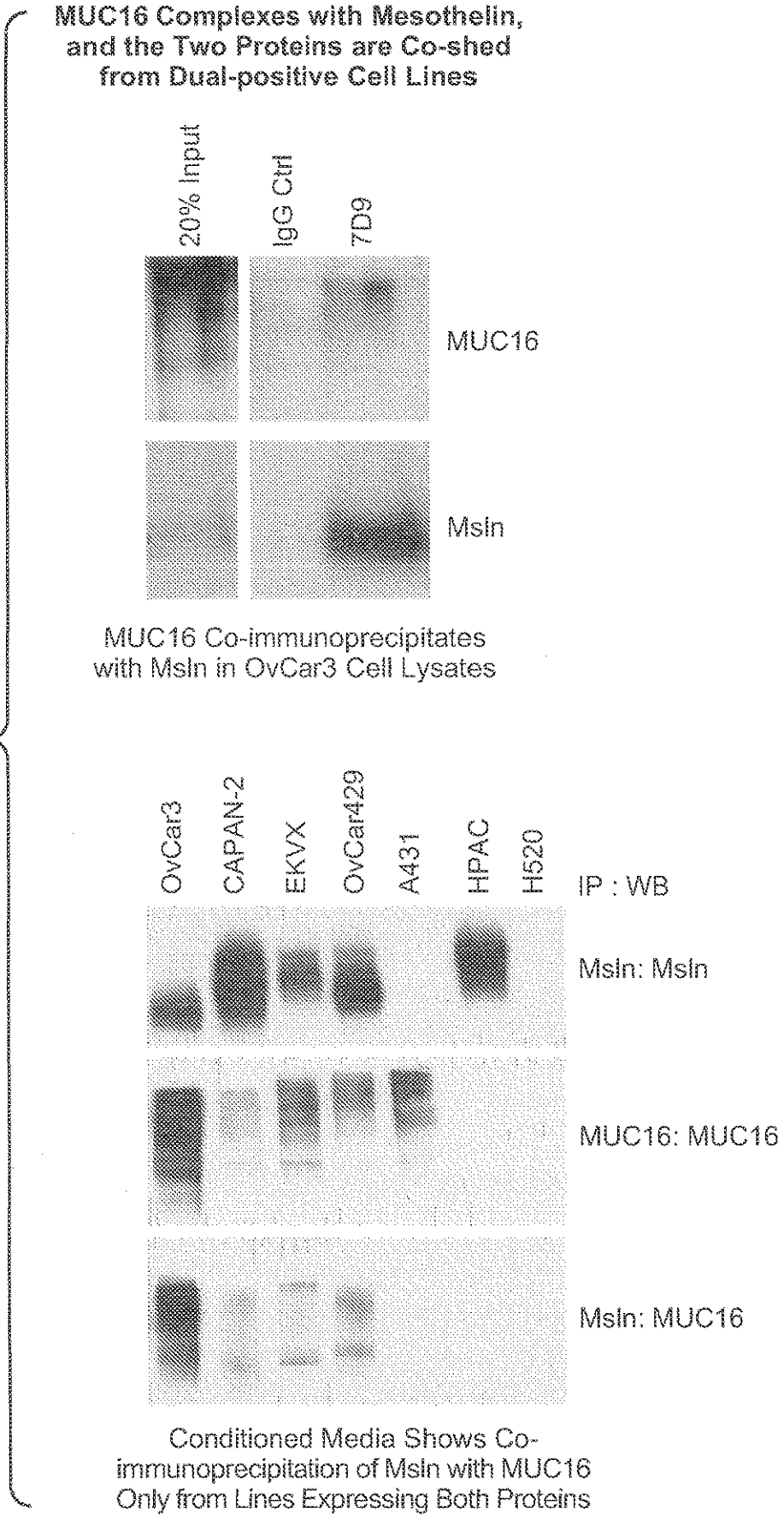

Efficacy of h7D9.v3-vcMMAE Similar to h22A10-vcMMAE
H226.x2 Mesothelioma Xenograft Model
Mean Tumor Volume (mm3) +/- SEM
1400
1200
1000
800
600
400
200
0
0
10
20
30
40
Day
Neg Control
(5 mg/kg)
Neg Control
(10 mg/kg)
Vehicle
5 mg/kg
h7D9.v3-VCE
5.0 mg/kg
h22A10.v83-VCE
10 mg/kg
h22A10.v83-VCE
10 mg/kg
h7D9.v3-VCE
IV:
PK:
OvCar3x2.1 Ovarian Xenograft Model
Mean Tumor Volume (mm3) +/- SEM
2000
1600
1200
800
400
0
0
10
20
30
40
Day
Neg Control
(6 mg/kg)
Vehicle
3 mg/kg
h7D9.v3-VCE
6 mg/kg
h22A10.v83-VCE
3 mg/kg
h22A10.v83-VCE
6 mg/kg
h7D9.v3-VCE
IV:
PK:

FIG. 31

FIG. 32


MUC16 Complexes with Mesothelin, and the Two Proteins are Co-shed from Dual-positive Cell Lines
20% Input
IgG Ctrl
7D9
MUC16
MsIn
MUC16 Co-immunoprecipitates with MsIn in OvCar3 Cell Lysates
OvCar3
CAPAN-2
EKVX
OvCar429
A431
HPAC
H520
IP : WB
MsIn: MsIn
MUC16: MUC16
MsIn: MUC16
Conditioned Media Shows Co-immunoprecipitation of MsIn with MUC16 Only from Lines Expressing Both Proteins

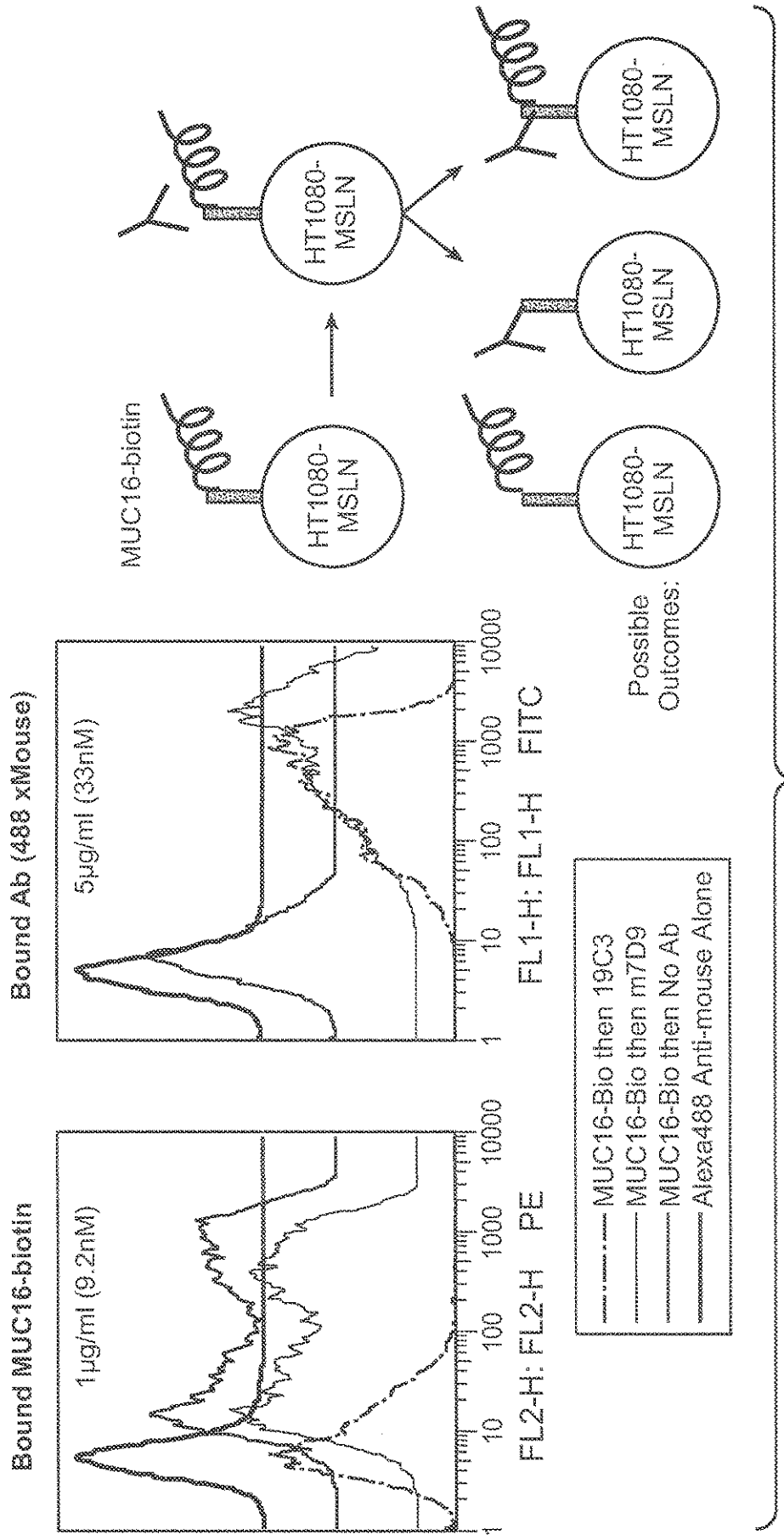

Bound MUC16-biotin
1µg/ml (9.2nM)
FL2-H: FL2-H PE
Bound Ab (488 xMouse)
5µg/ml (33nM)
FL1-H: FL1-H FITC
MUC16-Bio then 19C3
MUC16-Bio then m7D9
MUC16-Bio then No Ab
Alexa488 Anti-mouse Alone
MUC16-biotin
HT1080-MSLN
Possible Outcomes:
HT1080-MSLN
HT1080-MSLN
HT1080-MSLN

FIG. 33